Inorganic Chemistry

Article

pubs.acs.org/IC

Synthesis and Lanthanide Coordination Chemistry of Phosphine Oxide Decorated Dibenzothiophene and Dibenzothiophene Sulfone Platforms

Daniel Rosario-Amorin,[†] Sabrina Ouizem,[†] Diane A. Dickie,[†] Robert T. Paine,*[,†] Roger E. Cramer,[‡] Benjamin P. Hay,[§] Julien Podair,[§] and Lætitia H. Delmau[§]

[†]Department of Chemistry and Chemical Biology, University of New Mexico, Albuquerque, New Mexico 87131, United States

[‡]Department of Chemistry, University of Hawaii, Honolulu, Hawaii 96822, United States

[§]Chemical Sciences Division, Oak Ridge National Laboratory, P.O. Box 2008, Oak Ridge, Tennessee 37831, United States

Supporting Information

ABSTRACT: Syntheses for new ligands based upon dibenzothiophene and dibenzothiophene sulfone platforms, decorated with phosphine oxide and methylphosphine oxide donor groups, are described. Coordination chemistry of 4,6-bis(diphenylphosphinoylmethyl)dibenzothiophene (**8**), 4,6-bis(diphenylphosphinoylmethyl)dibenzothiophene-5,5-dioxide (**9**) and 4,6-bis(diphenylphosphinoyl)dibenzothiophene-5,5-dioxide (**10**) with lanthanide nitrates, $Ln(NO_3)_3{\cdot}(H_2O)_n$ is outlined, and crystal structure determinations reveal a range of chelation interactions on Ln(III) ions. The nitric acid dependence of the solvent extraction performance of **9** and **10** in 1,2-dichloroethane for Eu(III) and Am(III) is described and compared against the extraction behavior of related dibenzofuran ligands (**2**, **3**; R = Ph) and *n*-octyl(phenyl)-*N*,*N*-diisobutylcarbamoylmethyl phosphine oxide (**4**) measured under identical conditions.

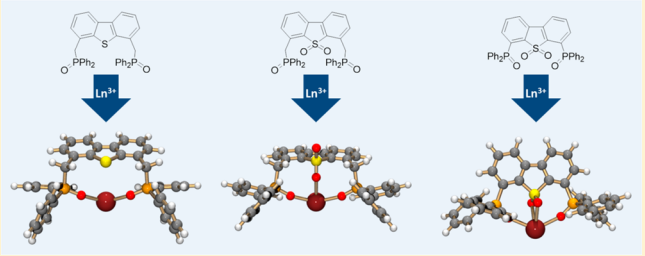

INTRODUCTION

A large number of organic molecules have been used as platforms to append and organize donor groups such that the resulting functionalized molecules behave as chelating ligands toward metal ions. The fundamental coordination properties of such ligands have been extensively studied, and practical applications for the ligands and their complexes are numerous. As examples, we have recently reported on the use of 2-pyridine *N*-oxide, [2-(X)C_5H_4NO], and 2,6-pyridine *N*-oxide, [2,6-$(X)_2C_5H_3NO$], platforms to prepare chelating ligands decorated with functional arms X = phosphine oxide, $-[P(O)R_2]$,[1,2] phosphonate, $-[P(O)(OR)_2]$,[3] methylphosphine oxide, $-[CH_2P(O)R_2]$,[4−13] methylphosphonate, $-[CH_2P(O)(OR)_2]$,[14] methylphosphinic acid, $-CH_2P(O)(OH)_2$],[14] methylphosphine sulfide, $-[CH_2P(S)R_2]$,[15] and methylamido, $-[CH_2C(O)N(H)R]$[16] and $-[CH_2CH_2C(O)NR_2]$.[17] These ligands generally favor binding with hard lanthanide cations; the 2-(X)C_5H_4NO compounds adopt bidentate, O_NO_P,[4,13] or O_NO_C[17] chelate interactions, while the 2,6-$(X)_2C_5H_3NO$ compounds bond as tridentate $O_PO_NO'_{P'}$[11−17] or $O_CO_NO'_{C'}$ chelates. In turn, favorable solubility and binding/release thermodynamic and kinetic features for several of the $O_PO_NO'_{P'}$-class ligands and complexes support interesting solvent extraction performance for trivalent f-block element cations in acidic aqueous solutions.[18−21]

Furan and dibenzofuran platforms have also been used in the past to derive multifunctional chelating ligands, and, in particular, the rigid 4,6-bis(X)$_2$dibenzofuran, [4,6-$(X)_2$DBF, **1**], fragment has been used to form acyclic[22−35] and macrocyclic[36−40] ligands decorated primarily with soft donor groups incorporated in the X substituents. The coordination chemistry of these ligands has not been extensively explored, but in some complexes the DBF O atom participates in chelate formation,[23,24,27,33,35] while in other complexes it does not.[25,28−30] Recently, with very different goals in mind, the decoration of the 4,6-$(X)_2$DBF platform with hard diphenylphosphine oxide fragments was accomplished.[41,42] Han and coworkers[41] prepared and studied 4,6-bis(diphenylphosphinoyl)-dibenzofuran (**2**, R = Ph) as a host for blue and green electrophosphorescence materials, while we prepared and explored the chelation properties of this molecule and the related 4,6-bis(diphenylphosphinoylmethyl)dibenzofuran (**3**, R = Ph) with hard Ln(III) and Pu(IV) ions.[42] Bidentate $O_PO'_{P'}$ binding was structurally confirmed in several isolated complexes of **2** and **3**, but no examples of tridentate $O_PO_{furan}O'_{P'}$ binding were observed. This preference parallels the expected weak donor strength of the furan O atom as well as ligand strain analysis[42] that compared both the energetics of tridentate $O_PO_{furan}O'_{P'}$ versus bidentate $O_PO'_{P'}$ structures formed by **2** and **3** and the donor bond vector convergence in tridentate and bidentate structures. Consistent with the

Received: February 27, 2014
Published: May 20, 2014

   dx.doi.org/10.1021/ic500471w | *Inorg. Chem.* 2014, 53, 5698−5711

modeling analyses, it was also deduced from solvent extraction data that **2** (R = Ph) is a better extractant toward Am(III) and Eu(III) than **3** (R = Ph) and that **2** is comparable in extraction performance to the commercial extractant *n*-octyl(phenyl)-*N*,*N*-diisobutylcarbamoylmethylphosphine oxide (OΦDi-BCMPO, **4**).[43]

In efforts to extend their studies of optoelectronic properties, Han and co-workers[44] recently reported a synthesis for the 4,6-dibenzothiophene (X_2DBT) analogue of **2**, 4,6-bis-(diphenylphosphinoyl)dibenzothiophene, and they examined the impact of this substitution on electron injection and transportation. Extending our prior studies of the coordination behavior of X_2DBF platform ligands **2** and **3** on Ln(III) ions, we report here syntheses for the DBT analogue of **3**, 4,6-bis(diphenylphosphinoylmethyl)dibenzthiophene, its sulfone derivative and the sulfone derivative of 4,6-bis-(diphenylphosphinoyl)dibenzothiophene, selected coordination chemistry with Ln(III) ions, and initial characterization of the solvent extraction behavior of the sulfone derivatives.

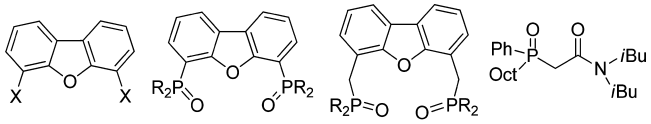

1 **2** **3** **4**

EXPERIMENTAL SECTION

General Information. Organic reagents (Aldrich Chemical) and metal nitrates (Ventron) were used as received, and organic solvents (VWR) were dried and distilled by standard methods. Reactions were performed under dry nitrogen unless specified otherwise. Infrared (IR) spectra were recorded on a Bruker Tensor 27 benchtop spectrometer. Solution NMR spectra were recorded with Bruker Avance-300 and -500 multinuclear spectrometers using Me_4Si (^1H, ^{13}C) and 85% H_3PO_4 (^{31}P) as external standards. Downfield shifts from the reference resonances were given $+\delta$ values.[45] Mass spectra for the ligands were obtained from the University of New Mexico Mass Spectrometry Center by using electrospray ionization (ESI) with a Waters/Micromass mass spectrometer operating in the positive ion mode. Elemental analyses were performed by Galbraith Laboratories.

Ligand Syntheses. *4,6-Diformyldibenzothiophene (**5**).* The compound was prepared in a fashion similar to that described in the literature.[46] A solution of dibenzothiophene (5.00 g, 27.1 mmol) and *N*,*N*,*N*′,*N*′-tetramethylethylene diamine (TMEDA) (10.1 mL, 67.8 mmol) in dry hexane (150 mL) was cooled (0 °C) under nitrogen atmosphere, and a solution of *n*-BuLi (1.6 M in hexane, 42.4 mL, 67.8 mmol) was added dropwise over 30 min. The resulting mixture was refluxed (15 min), then cooled (0 °C), and dimethylformamide (DMF) (12.6 mL, 163 mmol) was added. The mixture was allowed to slowly warm (23 °C, 1 h) while being stirred and was then poured onto an ice bath. A precipitate formed that was collected by filtration, washed with water (3 × 50 mL), and recrystallized from toluene leaving **5** as a white powder: yield 3.17 g, 49%; melting point (mp) 238−240 °C. ^1H NMR (300 MHz, $CDCl_3$): δ 10.36 (s, 2H, H_1), 8.51 (d, J_{HH} = 7.8 Hz, 2H, H_5), 8.08 (d, J_{HH} = 7.5 Hz, 2H, H_3), 7.75 (t, J_{HH} = 7.6 Hz, 2H, H_4). $^{13}C\{^1H\}$ NMR (75.5 MHz, $CDCl_3$): δ 191.20 (C_1), 140.72 (C_7), 135.67 (C_6), 133.48 (C_5), 131.40 (C_2), 127.04 (C_3), 125.02 (C_4). Fourier transform infrared (FTIR) (KBr, cm^{-1}): 2846, 2827, 1684, 1560, 1461, 1429, 1385, 1328, 1218, 1183, 996, 874, 776. High-resolution mass spectrometry (HRMS) (ESI): *m*/*z* (%): 241.0331 (52) [M + H^+]. $C_{14}H_9O_2S$ requires 241.0323; 263.0153 (100) [M + Na^+]. $C_{14}H_8O_2SNa$ requires 263.0143.

*4,6-Bis(hydroxymethyl)dibenzothiophene (**6**).* The procedure for conversion of **5** to **6** is similar to that provided in the literature.[46] To a suspension of **5** (3.10 g, 12.9 mmol) in MeOH/$CHCl_3$ (1/1, 80 mL) was added $NaBH_4$ (1.46 g, 38.7 mmol), and the mixture was stirred (23 °C, 2 h) under nitrogen. The resulting mixture was concentrated to 10 mL, and water (30 mL) was added. The precipitate formed was collected by filtration and washed with cold ethanol and CH_2Cl_2 to give **6** as a white powder: yield 2.90 g, 92%; mp 216−218 °C. ^1H NMR (300 MHz, d_6-dimethyl sulfoxide (DMSO)): δ 8.26 (d, J_{HH} = 5.1 Hz, 2H, H_5), 7.52 (m, 4H, $H_{3,4}$), 5.57 (s, 2H, O*H*) 4.80 (s, 4H, H_1). $^{13}C\{^1H\}$ NMR (75.5 MHz, d_6-DMSO): δ 136.53 (C_7), 136.43 (C_6), 135.38 (C_2), 124.66 (C_4), 124.50 (C_3), 120.62 (C_5), 62.24 (C_1). FTIR (KBr, cm^{-1}): 1484, 1426, 1349, 1324, 1245, 1173, 1135, 1078, 1060, 1036, 765. HRMS(ESI): *m*/*z* (%): 227.0531 (92) [M − (OH)$^+$]. $C_{14}H_{11}OS$ requires 227.0531; 267.0461 (100) [M + Na^+]. $C_{14}H_{12}O_2SNa$ requires 267.0456; 511.1023 (97) [2 M + Na^+]. $C_{28}H_{24}O_4S_2Na$ requires 511.1014.

*4,6-Bis(chloromethyl)dibenzothiophene (**7**).* A suspension of **6** (3.05 g, 12.5 mmol) and triphenylphosphine (9.82 g, 37.5 mmol) in dry CH_2Cl_2 (100 mL) was cooled (0 °C), and *N*-chlorosuccinimide (5.00 g, 37.5 mmol) was added with stirring. The temperature was maintained at 0 °C until the mixture became homogeneous, and then the solution was warmed (23 °C) and stirred (12 h). The resulting solution was washed with water (3 × 25 mL), dried (anhydrous $MgSO_4$), and filtered, and the solvent was vacuum evaporated. The brown residue obtained was purified by column chromatography (silica gel, eluted with hexane/CH_2Cl_2 70:30) leaving **7** as a pale yellow powder: yield 2.42 g, 69%; mp 184−186 °C. ^1H NMR (300 MHz, $CDCl_3$): δ 8.15 (dd, J_{HH} = 7.2, 1.6 Hz, 2H, H_5), 7.56−7.48 (m, 4H, $H_{3,4}$), 4.92 (s, 4H, H_1). $^{13}C\{^1H\}$ NMR (75.5 MHz, $CDCl_3$): δ 138.94 (C_7), 136.61 (C_6), 131.75 (C_2), 127.67 (C_3), 125.30 (C_4), 122.27 (C_5), 45.21 (C_1). FTIR (KBr, cm^{-1}): 1444, 1425, 1388, 1314, 1264, 1239, 1170, 1147, 1095, 1045, 976, 783, 759, 730, 677. HRMS(ESI): *m*/*z* (%): 302.9771 (86) [M + Na^+]. $C_{14}H_{10}Cl_2SNa$ requires 302.9778; 318.9508 (100) [M + K^+]. $C_{14}H_{10}Cl_2SK$ requires 318.9517.

*4,6-Bis(diphenylphosphinoylmethyl)dibenzothiophene (**8**).* A solution of **7** (1.08 g, 3.84 mmol) in ethyl diphenylphosphinite (4.90 mL, 22.7 mmol) was heated at 140 °C (14 h). After cooling (23 °C), the resulting white residue was collected and washed with diethyl ether (4 × 30 mL) giving **8** as a white powder: yield 2.27 g, 97%; mp 284−286 °C. $^{31}P\{^1H\}$ NMR (121.5 MHz, $CDCl_3$): δ 30.1. $^{31}P\{^1H\}$ NMR (121.5 MHz, d_4-MeOH): δ 34.4. ^1H NMR (300 MHz, $CDCl_3$): δ 7.94 (d, J_{HH} = 7.6 Hz, 2H, H_5), 7.76 (dd, J_{HH} = 11.2 Hz, 7.3 Hz, 8H, H_9), 7.53−7.38 (m, 14H, $H_{3,10,11}$), 7.29 (t, J_{HH} = 7.5 Hz, 2H, H_4), 3.90 (d, J_{HP} = 13.2 Hz, 4H, H_1). ^1H NMR (300 MHz, d_4-MeOH): δ 8.03 (d, J_{HH} = 7.8 Hz, 2H, H_5), 7.79 (dd, J_{HH} = 11.7 Hz, 7.8 Hz, 8H, H_9), 7.60−7.50 (m, 12H, $H_{10,11}$), 7.32−7.22 (m, 4H, $H_{3,4}$), 4.07 (d, J_{HP} = 13.5 Hz, 4H, H_1). $^{13}C\{^1H\}$ NMR (75.5 MHz, $CDCl_3$): δ 140.17 (d, J_{CP} = 6.6 Hz, C_7), 136.41 (C_6), 132.42 (d, J_{CP} = 99.8 Hz, C_8), 132.01 (C_{11}), 131.19 (d, J_{CP} = 9.4 Hz, C_9), 128.63 (d, J_{CP} = 11.7 Hz, C_{10}), 128.26 (d, J_{CP} = 4.3 Hz, C_3), 126.30 (d, J_{CP} = 7.5 Hz, C_2), 124.97 (C_4), 120.47 (C_5), 36.98 (d, J_{CP} = 67.3 Hz, C_1). FTIR (KBr, cm^{-1}): 2933, 1437, 1388, 1188 ($\nu_{P=O}$), 1119, 1030, 852, 836, 783, 757, 741, 723, 693, 555, 536, 514. HRMS(ESI): *m*/*z* (%): 613.1526 (35) [M + H^+]. $C_{38}H_{31}O_2P_2S$ requires 613.1520; 635.1353 (100) [M + Na^+]. $C_{38}H_{30}O_2P_2SNa$ requires 635.1339; 651.1081 (12) [M + K^+]. $C_{38}H_{30}O_2P_2SK$ requires 651.1071. Anal. Calcd for $C_{38}H_{30}O_2P_2S$: C 74.50, H 4.94, P 10.11. Found: C 74.26, H 4.96, P 9.75%.

*4,6-Bis(diphenylphosphinoylmethyl)dibenzothiophene-5,5-dioxide (**9**).* To a solution of **8** (1.10 g, 1.79 mmol) in dry CH_2Cl_2 (20 mL) was slowly added 3-chloroperoxybenzoic acid (77 wt %, 1.60 g, 7.14 mmol). The mixture was stirred (23 °C, 12 h); the resulting mixture was diluted with additional CH_2Cl_2 (100 mL) and washed with aqueous NaOH (2N, 3 × 25 mL) and distilled water (2 × 25 mL). The organic phase was dried (anhydrous $MgSO_4$) and filtered, and the volatiles were removed by vacuum evaporation, leaving a white powder, **9**: yield 1.10 g, 95%; mp 278−280 °C. $^{31}P\{^1H\}$ NMR (121.5 MHz, $CDCl_3$): δ 30.7. $^{31}P\{^1H\}$ NMR (121.5 MHz, d_4-MeOH): δ 34.0. ^1H NMR (300 MHz, $CDCl_3$): δ 8.11 (d, J_{HH} = 7.5 Hz, 2H, H_5), 7.88−7.81 (m, 8H, H_9), 7.53−7.42 (m, 16H, $H_{3,4,10,11}$), 4.11 (d, J_{HP} = 13.8 Hz, 4H, H_1). ^1H NMR (300 MHz, d_4-MeOH): δ 7.84−7.77 (m, 10H, $H_{5,9}$), 7.65−7.49 (m, 16H, $H_{3,4,10,11}$), 4.21 (d, J_{HP} = 13.8 Hz, 4H, H_1).

dx.doi.org/10.1021/ic500471w | Inorg. Chem. 2014, 53, 5698−5711

Table 1. Crystallographic Data for Ligands 8, 9·2CH_2Cl_2, and 10·3$CHCl_3$

	8	9·2CH_2Cl_2	10·3$CHCl_3$
empirical formula	$C_{38}H_{30}O_2P_2S$	$C_{40}H_{34}Cl_4O_4P_2S$	$C_{39}H_{29}Cl_9O_4P_2S$
crystal size (mm)	0.15 × 0.25 × 0.48	0.18 × 0.20 × 0.27	0.16 × 0.22 × 0.53
formula weight	612.62	814.47	974.67
crystal system	orthorhombic	triclinic	monoclinic
space group	*P*2(1)2(1)2(1) (No. 18)	*P*1 (No. 1)	*P*2(1)/*n* (No. 14)
unit cell dimen.			
a (Å)	5.7594(6)	8.9081(4)	14.6937(5)
b (Å)	16.772(2)	10.2099(5)	15.6122(5)
c (Å)	31.593(4)	11.4562(5)	20.4382(6)
α (deg)	90	91.404(3)	90
β(deg)	90	97.115(3)	94.086(2)
γ (deg)	90	114.544(3)	90
V (Å^3)	3051.8(6)	937.17(7)	4676.6(3)
Z	4	1	4
T (K)	173(2)	173(2)	173(2)
D_{cald} (g cm^{-3})	1.333	1.443	1.384
μ (mm^{-1})	0.245	0.499	0.689
min/max transmission	0.892/0.964	0.878/0.914	0.660/0.900
reflection collected	32 159	21 422	40 502
independent reflections [R_{int}]	6722 [0.1349]	8828 [0.0392]	9193 [0.0910]
final *R* indices [$I > 2\sigma(I)$] *R*1[a] (*wR*2)[b]	0.0560(0.1046)[c]	0.0395(0.0759)[d]	0.0807(0.2450)
final *R* indices (all data) *R*1 (*wR*2)	0.1012(0.1229)	0.0505(0.0822)	0.2450(0.3070)

[a]$R1 = (\Sigma||F_o| - |F_c||)/\Sigma|F_o|$. [b]$wR2 = [\Sigma w(F_o^2 - F_c^2)^2/\Sigma w(F_o^2)^2]^{1/2}$. [c]Flack parameter = 0.04(9). [d]Flack parameter = 0.03(4).

$^{13}C\{^1H\}$ NMR (75.5 MHz, $CDCl_3$): δ 135.34 (d, J_{CP} = 8.4 Hz, C_7), 134.03 (C_4), 132.34 (d, J_{CP} = 4.4 Hz, C_3), 132.16 (C_{11}), 131.80 (d, J_{CP} = 103.4 Hz, C_8), 131.75 (C_6), 131.17 (d, J_{CP} = 9.4 Hz, C_9), 130.57 (d, J_{CP} = 6.3 Hz, C_2), 128.74 (d, J_{CP} = 12.1 Hz, C_{10}), 120.16 (C_5), 31.98 (d, J_{CP} = 66.8 Hz, C_1). FTIR (KBr, cm^{-1}): 3072, 2904, 1587, 1480, 1435, 1288 ($\nu_{S=O(as)}$), 1211, 1194 ($\nu_{P=O}$), 1157 ($\nu_{S=O(sy)}$), 1119, 997, 824, 796, 754, 722, 695, 628, 592, 573, 524, 509, 474. HRMS(ESI): *m*/*z* (%): 645.1423 (46) [M + H$^+$]. $C_{38}H_{31}O_4P_2S$ requires 645.1418; 667.1246 (100) [M + Na$^+$]. $C_{38}H_{30}O_4P_2SNa$ requires 667.1238.

*4,6-Bis(diphenylphosphinoyl)dibenzothiophene-5,5-dioxide (**10**).* A solution of dibenzothiophene (3.00 g, 16.3 mmol) and TMEDA (6.75 mL, 45.3 mmol) in dry hexane (100 mL) was cooled (0 °C) under nitrogen atmosphere, and a solution of *n*-BuLi (1.6 M in hexane, 28.4 mL, 45.4 mmol) was added dropwise with stirring. The resulting mixture was refluxed (15 min), then cooled (0 °C), and a solution of chlorodiphenylphosphine (5.80 mL, 32.5 mmol) in hexane (40 mL) was added dropwise over 40 min. The mixture was stirred (23 °C, 12 h), then quenched with water (100 mL), and extracted with CH_2Cl_2 (3 × 100 mL). The organic layer was dried (anhydrous $MgSO_4$) and filtered, and the solvent was removed under vacuum. The brown residue obtained was washed with Et_2O (3 × 50 mL) leaving a yellow powder, which was then dissolved in dry CH_2Cl_2 (100 mL). The solution was cooled (0 °C), and 3-chloroperoxybenzoic acid (77 wt %, 21.9 g, 97.7 mmol) was added slowly. The mixture was stirred (23 °C, 4 h); the resulting mixture was diluted with additional CH_2Cl_2 (100 mL) and washed with aqueous NaOH (2N, 3 × 25 mL) and distilled water (2 × 25 mL). The organic phase was dried (anhydrous $MgSO_4$) and filtered, and the volatiles were removed by vacuum evaporation. The pale yellow residue obtained was purified by column chromatography (silica gel, eluted with CH_2Cl_2/MeOH 97:3) leaving **10** as a white powder: yield 4.90 g, 49%; mp > 380 °C decomposition. $^{31}P\{^1H\}$ NMR (121.5 MHz, $CDCl_3$): δ 27.7. $^{31}P\{^1H\}$ NMR (121.5 MHz, d_4-MeOH): δ 32.0. ^1H NMR (300 MHz, $CDCl_3$): δ 7.98 (d, J_{HH} = 6.0 Hz, 2H, H_4), 7.85−7.62 (m, 12H, $H_{2,3,8}$), 7.55−7.50 (m, 4H, H_{10}), 7.45−7.37 (m, 8H, H_9). ^1H NMR (300 MHz, d_4-MeOH): δ 8.34 (d, J_{HH} = 6.0 Hz, 2H, H_4), 7.76 (m, 2H, H_3), 7.63−7.43 (m, 22H, $H_{2,8,9,10}$). $^{13}C\{^1H\}$ NMR (75.5 MHz, $CDCl_3$): δ 140.55 (C_6), 135.82 (d, J_{CP} = 8.5 Hz, C_2), 132.98 (C_3), 132.77 (d, J_{CP} = 10.1 Hz, C_8), 132.41 (C_{10}), 131.49 (d, J_{CP} = 107.5 Hz, C_7), 131.31 (d, J_{CP} = 78.1 Hz, C_1), 129.81 (d, J_{CP} = 41.3 Hz, C_5), 128.46 (d, J_{CP} = 12.7 Hz, C_9), 124.94 (d, J_{CP} = 10.6 Hz, C_4). FTIR (KBr, cm^{-1}): 1573, 1483, 1437, 1414, 1331 ($\nu_{S=O(as)}$), 1196 ($\nu_{P=O}$), 1159 ($\nu_{S=O(s)}$), 1119, 1104, 1070, 855, 797, 752, 736, 723, 692, 591, 580, 549, 493. HRMS(ESI): *m*/*z* (%): 617.1121 (39) [M + H$^+$]. $C_{36}H_{27}O_4P_2S$ requires 617.1105; 639.0938 (100) [M + Na$^+$]. $C_{36}H_{26}O_4P_2SNa$ requires 639.0925; 655.0678 (20) [M + K$^+$]. $C_{36}H_{26}O_4P_2SK$ requires 655.0664.

Lanthanide Complex Syntheses. The lanthanide coordination complexes were prepared by combination of 1 equiv of ligand (50−100 mg) with 1 equiv of $Ln(NO_3)_3{\cdot}xH_2O$ in MeOH. The mixtures were stirred (23 °C, 1 h); volatiles were removed by vacuum evaporation, and the resulting powders were vacuum-dried. Elemental analyses (CHN) and IR spectra for representative samples were obtained, and selected samples were crystallized to obtain single crystals for X-ray diffraction analyses. *[La(**8**)(NO$_3$)$_3$]:* $^{31}P\{^1H\}$ NMR (121.5 MHz, d_4-MeOH): δ 36.2. ^1H NMR (300 MHz, d_4-MeOH): δ 8.03 (d, J_{HH} = 7.9 Hz, 2H, H_5), 7.79 (dd, J_{HH} = 11.4 Hz, 7.8 Hz, 8H, H_9), 7.62−7.51 (m, 12H, $H_{10,11}$), 7.25 (t, J_{HH} = 7.5 Hz, 2H, H_4), 7.08 (d, J_{HH} = 7.2 Hz, 2H, H_3), 4.13 (d, J_{HP} = 13.2 Hz, 4H, H_1). FTIR (KBr, cm^{-1}): 1240 (ν_{PO}). *[Pr(**8**)(NO$_3$)$_3$(H$_2$O)]:* FTIR (KBr, cm^{-1}): 1240 (ν_{PO}). Anal. Calcd for $C_{38}H_{32}N_3O_{12}P_2PrS$: C 47.66, H 3.37. Found C 48.31, H 3.63%. *[La(**9**)(NO$_3$)$_3$(H$_2$O)]:* $^{31}P\{^1H\}$ NMR (121.5 MHz, d_4-MeOH): δ 37.2. ^1H NMR (300 MHz, d_4-MeOH): δ 7.87−7.84 (m, 10H, $H_{5,9}$), 7.67−7.57 (m, 12H, $H_{10,11}$), 7.42 (t, J_{HH} = 7.8 Hz, 2H, H_4), 6.87 (m, 2H, H_3), 4.33 (d, J_{HP} = 13.2 Hz, 4H, H_1). FTIR (KBr, cm^{-1}): 1286 (br, $\nu_{SO(as)}$), 1155 (br, $\nu_{PO,}$ ν_{SO}). Anal. Calcd for $[C_{38}H_{30}LaN_3O_{13}P_2S]{\cdot}5H_2O$: C 43.07, H 3.80, N 3.97. Found C 43.03, H 3.51, N 3.75%. *[Pr(**9**)(NO$_3$)$_3$]*: FTIR (KBr, cm^{-1}): 1288 (br, $\nu_{SO(as)}$), 1151 (br, $\nu_{PO,}$ ν_{SO}). Anal. Calcd for $[C_{38}H_{30}N_3O_{13}P_2PrS]{\cdot}4H_2O$: C 43.73, H 3.67, N 4.03. Found C 43.74, H 3.33, N 3.85%. *[Eu(**9**)(NO$_3$)$_3$]*: FTIR (KBr, cm^{-1}): 1281 (br, $\nu_{SO(as)}$), 1151 (br, $\nu_{PO,}$ ν_{SO}). *[Dy(**9**)(NO$_3$)$_3$]*: FTIR (KBr, cm^{-1}): 1286 (br, $\nu_{SO(as)}$), 1155 (br, $\nu_{PO,}$ ν_{SO}). *[Er(**9**)(NO$_3$)$_3$]*: FTIR (KBr, cm^{-1}): 1288 (br, $\nu_{SO(as)}$), 1151 (br, $\nu_{PO,}$ ν_{SO}). *[Lu(**9**)(NO$_3$)$_3$]*: FTIR (KBr, cm^{-1}): 1284 (br, $\nu_{SO(as)}$), 1151 (br, $\nu_{PO,}$ ν_{SO}). *[La(**10**)(NO$_3$)$_3$]*: $^{31}P\{^1H\}$ NMR (121.5 MHz, d_4-MeOH): δ 34.5. ^1H NMR (300 MHz, d_4-MeOH): δ 8.41 (d, J_{HH} = 7.8 Hz, 2H, H_4), 7.86 (t, 2H, J_{HH} = 7.7 Hz, H_3), 7.69−7.62 (m, 12H, $H_{8,10}$), 7.54−7.41 (m, 10H, $H_{2,9}$). FTIR (KBr, cm^{-1}): 1311 (br, $\nu_{SO(as)}$), 1155 (br, ν_{SO}). *[Pr(**10**)(NO$_3$)$_3$]*: FTIR (KBr, cm^{-1}): 1305 (br, $\nu_{SO(as)}$), 1169 (br, ν_{PO}), 1151 (br, ν_{SO}). *[Eu(**10**)(NO$_3$)$_3$]*: FTIR (KBr, cm^{-1}): 1305 (br, $\nu_{SO(as)}$), 1155 (br, $\nu_{PO,}$ ν_{SO}). *[Dy(**10**)(NO$_3$)$_3$]*: FTIR

dx.doi.org/10.1021/ic500471w | *Inorg. Chem.* 2014, 53, 5698−5711

Table 2. Crystallographic Data for Coordination Complexes

	{[Pr(8)$(NO_3)_3$(MeCN)]·[Pr(8)$(NO_3)_3(H_2O)$]}·3MeCN	[La(9)$(NO_3)_3(H_2O)$]	[Er(9)$(NO_3)_3$]·2MeCN	{[Eu(9)$(Cl)_3]_2(\mu$-9)}·5MeCN	[Pr(10)$(NO_3)_3$$(MeOH)_2$]·MeOH
empirical formula	$C_{84}H_{74}N_{10}O_{23}P_4Pr_2S_2$	$C_{38}H_{32}LaN_3O_{14}P_2S$	$C_{42}H_{36}ErN_5O_{13}P_2S$	$C_{124}H_{105}Cl_6Eu_2N_5O_{12}P_6S_3$	$C_{39}H_{38}N_3O_{16}P_2PrS$
crystal size (mm)	0.23 × 0.24 × 0.39	0.14 × 0.26 × 0.29	0.21 × 0.28 × 0.45	0.18 × 0.22 × 0.32	0.33 × 0.49 × 0.49
formula weight	2061.35	987.58	1080.02	2655.74	1039.63
crystal system	triclinic	monoclinic	monoclinic	monoclinic	triclinic
space group	$P\bar{1}$ (No. 2)	$C2/c$ (No. 15)	$P2(1)/c$ (No. 14)	$P2(1)/n$ (No. 14)	$P\bar{1}$ (No. 2)
unit cell dimen.					
a (Å)	12.2302(4)	14.8649(11)	15.4086(8)	22.6280(7)	12.3875(3)
b (Å)	18.6944(6)	16.2720(13)	12.6936(5)	11.0181(4)	13.2484(3)
c (Å)	20.9282(8)	36.997(3)	23.8809(12)	48.6986(17)	14.9970(4)
α (deg)	93.358(2)	90	90	90	105.6510(10)
β (deg)	105.040(2)	91.016(4)	108.487(2)	97.762(2)	90.7990(10)
γ (deg)	104.222(2)	90	90	90	112.3280(10)
V (Å^3)	4441.0(3)	8947.5(12)	4429.8(4)	12030.2(7)	2173.47(9)
Z	2	8	4	4	2
T (K)	173(2)	173(2)	173(2)	173(2)	173(2)
D_{calcd} (g cm^{-3})	1.542	1.466	1.619	1.466	1.589
μ (mm^{-1})	1.282	1.138	2.084	1.360	1.316
min/max transmission	0.610/0.760	0.726/0.859	0.454/0.674	0.670/0.790	0.563/0.669
reflection collected	20 352	64 328	55 816	79 965	66 545
independent reflections [R_{int}]	20 329 [0.0559]	11 573 [0.0555]	11 428 [0.0345]	23 574 [0.0965]	16 435 [0.0171]
final R indices [$I > 2\sigma(I)$] $R1^a$ ($wR2$)^b	0.0504 (0.1234)	0.0526(0.1507)	0.0234(0.0525)	0.0560(0.1023)	0.0228(0.0614)
final R indices (all data) $R1$($wR2$)	0.0822(0.1343)	0.0694(0.1599)	0.0331(0.0570)	0.1098(0.1158)	0.0260(0.0639)

$^a R1 = (\Sigma||F_o| - |F_c||)/\Sigma|F_o|$. $^b wR2 = [\Sigma w(F_o^2 - F_c^2)^2/\Sigma w(F_o^2)^2]^{1/2}$.

dx.doi.org/10.1021/ic50047w | Inorg. Chem. 2014, 53, 5698−5711

Scheme 1

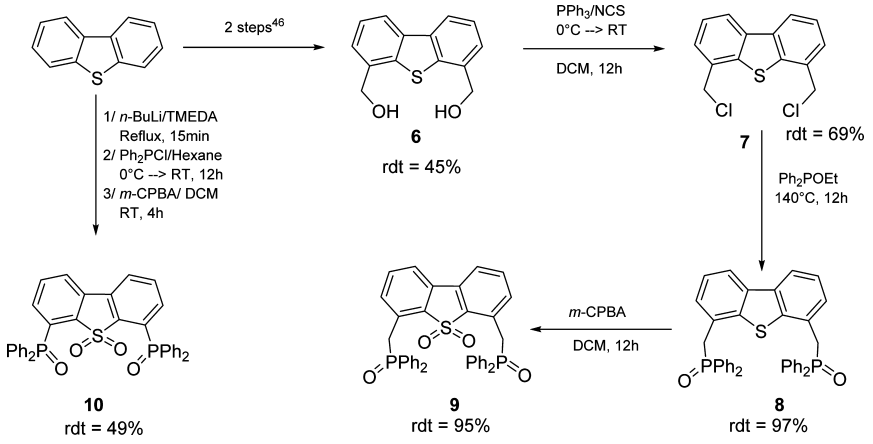

(KBr, cm^{-1}): 1300 (br, $\nu_{SO(as)}$), 1155 (br, $\nu_{PO,}$ ν_{SO}). *[Er(**10**)$(NO_3)_3$]*: FTIR (KBr, cm^{-1}): 1298 (br, $\nu_{SO(as)}$), 1155 (br, $\nu_{PO,}$ ν_{SO}). {[Eu(**9**)Cl_3]$_2$(μ-**9**)}·5(MeCN) was prepared by combination of $EuCl_3·6H_2O$ (28.4 mg, 1 equiv) with an excess of **9** (200 mg, 3 equiv) in MeOH (4 mL). The mixture was stirred (23 °C, 1 h), and volatiles were removed by vacuum evaporation leaving a colorless powder. Anal. Calcd for $C_{114}H_{90}Cl_6Eu_2O_{12}P_6S_3$: C 55.87, H 3.70. Found C 55.59, H 3.57%. FTIR (KBr, cm^{-1}): 1290 (br, $\nu_{SO(as)}$), 1157 (br, $\nu_{PO,}$ ν_{SO}). The colorless powder was recrystallized from MeCN/MeOH (9/1, 4 mL) by slow evaporation.

X-ray Diffraction Analyses. Crystals of the ligands and lanthanide complexes were coated with Paratone oil and mounted on a CryoLoop attached to a metal pin with epoxy. Diffraction data were collected with a Bruker X8 Apex II CCD-based X-ray diffractometer equipped with an Oxford Cryostream 700 low-temperature device and normal focus Mo-target X-ray tube (λ = 0.710 73 Å) operated at 1500 W power (50 kV, 30 mA). Data collection and processing were accomplished with the Bruker APEX2 software suite.[47] The structures were solved by direct methods and refined with full-matrix least-squares methods on F^2 with use of SHELXTL.[48] Lattice and data collection parameters for the ligands and the metal complexes are presented in Tables 1 and 2, respectively. All heavy atoms were refined anisotropically, and hydrogen atoms were included in ideal positions and refined isotropically (riding model) with U_{iso} = 1.2U_{eq} of the parent atom (U_{iso} = 1.5U_{eq} for methyl groups) unless noted otherwise. The structure refinements were well-behaved except as indicated in the following notes. Colorless rods of **8** were obtained by holding a MeOH/CH_2Cl_2 (2 mL, 95:5) solution of **8** (30 mg) at −20 °C (12 h). Colorless rods of **9**·2CH_2Cl_2 were obtained by holding a MeOH/CH_2Cl_2 (5 mL, 95:5) solution of **9** at −20 °C (12 h). Colorless rods of **10**·3$CHCl_3$ were obtained by slow evaporation of a $CDCl_3$ solution of **10** (50 mg) at 23 °C. The chlorine atom Cl8 is disordered over two sites, and the occupancies were allowed to refine freely. One molecule of $CHCl_3$ could not be acceptably modeled, and it was accounted for by using SQUEEZE.[49] Colorless blocks of [Pr(**8**)$(NO_3)_3$(MeCN)]·[Pr(**8**)$(NO_3)_3(H_2O)$]·3MeCN were formed by slow evaporation of a saturated MeCN/MeOH (4:1) solution. Colorless blocks of [La(**9**)$(NO_3)_3(H_2O)$] were obtained by slow evaporation of a MeCN/MeOH (9:1) solution. All atoms of one nitrate group, N3, O8, O9, O10, and one inner sphere molecule of water, O14, are disordered over two positions. Constraints on bond lengths and thermal displacement parameters were applied to the disordered species. Further disordered solvent was accounted for by using SQUEEZE.[49] Pink platelets of [Er(**9**)$(NO_3)_3$]·2MeCN were formed by slow evaporation of a MeCN/MeOH (9:1) solution. A colorless rod-like specimen was cut from a larger crystal of {[Eu(**9**)Cl_3]$_2$(μ-**9**)}·5(MeCN) obtained by slow evaporation of a MeCN/MeOH (9:1) solution. One of the five independent MeCN lattice solvent molecules was found disordered equally over two positions. The occupancy was freely refined with constraints on the anisotropic displacement parameters of the affected atoms. Colorless prisms of [Pr(**10**)$(NO_3)_3$-$(MeOH)_2$]·MeOH were obtained by slow evaporation of a MeCN/MeOH (9:1) solution.

Distribution Studies. All salts and solvents were reagent grade and were used as received. Extraction experiments were carried out using 1,2-dichloroethane (OmniSolv, EM Science) as the diluent. The aqueous phases were prepared using nitric acid (J. T. Baker, Ultrex II) and europium nitrate (Aldrich, 99.9%). Distilled, deionized water was obtained from a Barnstead Nanopure filter system (resistivity at least 18.2 MΩ cm) and used to prepare all the aqueous solutions. The radioisotope ^{241}Am was provided by the Radiochemical and Engineering Research Center of Oak Ridge National Laboratory. The radiotracer $^{152/154}$Eu was obtained from Isotope Products, Burbank, CA. Both were added as spikes to the aqueous phases in the sample equilibration vials in the extraction experiments.

Phases at a 1:1 organic to aqueous (O/A) phase ratio were combined in 2 mL polypropylene microtubes, which were then capped and mounted by clips on a disk that was rotated in a constant-temperature air box at 25.0 ± 0.5 °C for 1 h. After the contacting period, the tubes were centrifuged for 5 min at 3000 rpm and 25 °C in a Beckman Coulter Allegra 6R temperature-controlled centrifuge. A 250 μL aliquot of each phase was subsampled and counted using a Canberra Analyst pure Ge Gamma counter. Counting times were sufficient to ensure that counting error was a small fraction of the precision of the obtained distribution ratios, considered from a combination of volumetric, replicate, and counting errors to be ±5%. Americium and europium distribution ratios were calculated as the ratio of the volumetric count rates of the ^{241}Am and $^{152/154}$Eu isotopes in each phase at equilibrium.

Molecular Mechanics Calculations. Geometry optimizations of the free and metal-bound forms of **8**, **9**, and **10** were carried out with the MM3 force field[50] using a points-on-a-sphere metal ion[51] as implemented in PCModel software.[52] Conformational searches to locate the most stable form for each structure were performed using the GMMX algorithm provided with this software.

RESULTS AND DISCUSSION

Ligand Syntheses. The initial target DBT ligand, **8**, was prepared in four steps from dibenzothiophene following the pathway summarized in Scheme 1. The precursors 4,6-diformyldibenzothiophene, **5**, and 4,6-bis(hydroxymethyl)-dibenzothiophene, **6**, were prepared essentially as described in the literature[46] by a double formylation of dibenzothiophene followed by reduction with $NaBH_4$. The conversion of **6** to 4,6-bis(chloromethyl)dibenzothiophene, **7**, was accomplished in a manner similar to the procedure described previously for the preparation of 4,6-bis(chloromethyl)dibenzofuran.[42] Lastly, the initial target, 4,6-bis(diphenylphosphinoylmethyl)-dibenzothiophene, **8**, was obtained with 97% yield from an

dx.doi.org/10.1021/ic500471w | Inorg. Chem. 2014, 53, 5698−5711

Arbuzov reaction of **7** with Ph_2POEt. The composition of **8** is supported by elemental analysis (CHP), and HRMS analysis shows high-intensity $[M + H^+]$, $[M + Na^+]$, and $[M + K^+]$ ions. The FTIR spectrum of **8** contains a strong absorption at 1188 cm^{-1} that is assigned to a $\nu_{P=O}$ stretching mode, and the ^{31}P NMR spectrum displays a single resonance that is solvent dependent: δ 30.1 ($CDCl_3$); 34.4 (d_4-MeOH). These shifts are comparable to those reported for 4,6-bis-(diphenylphosphinoylmethyl)dibenzofuran, **3** (R = Ph): δ 29.8 ($CDCl_3$); 34.5 (d_4-MeOH).[42] The ^1H and ^{13}C NMR spectra ($CDCl_3$) are consistent with the proposed structure, and the shifts for the methylene group are noteworthy: H_1, δ 3.90 (J_{HP} = 13.2 Hz), C_1, δ 36.98 (J_{HP} = 67.3 Hz). The molecular structure of **8** was confirmed by single-crystal X-ray diffraction analysis. A view of the molecule is shown in Figure 1,

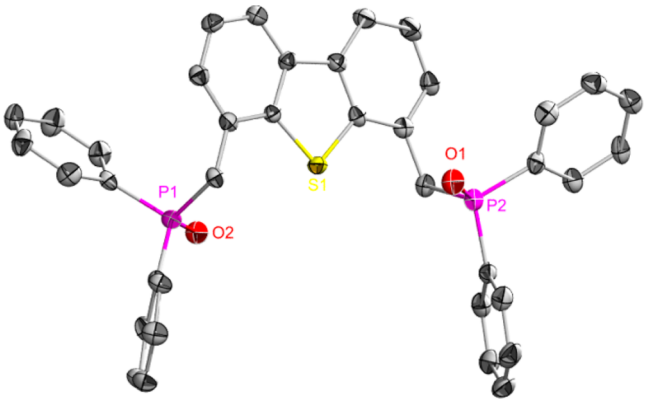

Figure 1. Molecular structure of 4,6-$[Ph_2P(O)CH_2]_2$DBT, **8**, (thermal ellipsoids, 50%) with carbon atom labels and H atoms omitted for clarity.

Table 3. Selected Bond Lengths for Ligands 8, 9·2CH_2Cl_2, and 10·3$CHCl_3$

bond type	8	9·2CH_2Cl_2	10·3$CHCl_3$
P–O	P1–O2 1.493(3)	P1–O1 1.494(2)	P1–O1 1.485(4)
	P2–O1 1.490(3)	P2–O2 1.484(2)	P2–O2 1.491(4)
S–O		S1–O3 1.439(2)	S1–O3 1.439(4)
		S1–O4 1.437(2)	S1–O4 1.439(4)
P–$C_{(CH2\ or\ DBT)}$	P1–C5 1.817(3)	P1–C13 1.838(2)	P1–C10 1.821(6)
	P2–C10 1.829(4)	P2–C26 1.823(3)	P2–C25 1.822(6)
S–C	S1–C7 1.758(4)	S1–C11 1.767(2)	S1–C11 1.785(5)
	S1–C8 1.753(4)	S1–C12 1.771(3)	S1–C12 1.790(5)

and selected bond lengths are given in Table 3. The dibenzothiophene backbone is planar, and the P=O bond vectors are rotated out of the backbone plane in opposite directions. The average (av) P=O bond length, 1.491 ± 0.002 Å, is indistinguishable from that reported for the furan analogue **3** (R = Ph), 1.491 ± $0.003_{(av)}$ Å.[42]

S-Oxidation of **8** with an excess of meta-chloroperoxybenzoic acid (*m*-CPBA) at room temperature gave 4,6-bis-(diphenylphosphinoylmethyl)dibenzothiophene sulfone, **9**, with 95% yield. The composition of **9** is supported by a HRMS that shows high-intensity $[M + H^+]$ and $[M + Na^+]$ ions. The FTIR spectrum displays strong absorptions tentatively assigned to $\nu_{S=O(as)}$, $\nu_{P=O}$, and $\nu_{S=O(s)}$ stretching vibrations at 1288, 1194, and 1157 cm^{-1}, respectively. The ^{31}P NMR spectrum contains a single, solvent-dependent resonance: δ 30.7 ($CDCl_3$); 34.0 (d_4-MeOH). These resonances are slightly shifted from the resonances for the precursor **8**. The ^1H and ^{13}C NMR spectra ($CDCl_3$) are also consistent with the proposed structure. Notably, the proton and carbon resonances assigned to the methylene groups spanning the $DBT(O)_2$ ring and the phosphine oxide group, H_1, δ 4.11 (J_{HP} = 13.8 Hz) and C_1, δ 31.98 (J_{HP} = 66.8 Hz), are significantly shifted from the respective resonances for **8**. The molecular structure of **9**, cocrystallized with two molecules of CH_2Cl_2, was determined by single-crystal X-ray diffraction analysis. A view of the molecule is shown in Figure 2, and selected bond lengths are

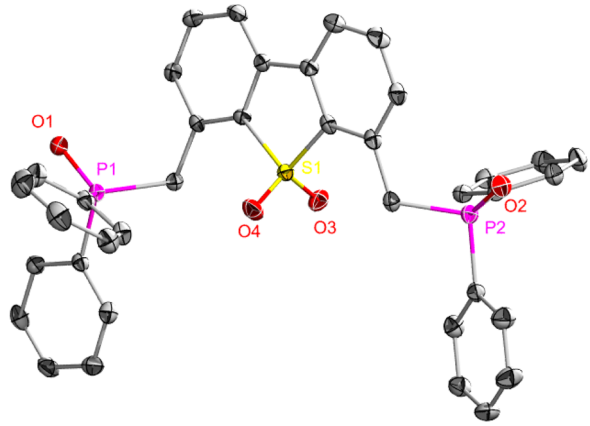

Figure 2. Molecular structure of 4,6-$[Ph_2P(O)CH_2]_2DBT(O)_2$·$2CH_2Cl_2$, **9**·$2CH_2Cl_2$ (thermal ellipsoids, 50%) with carbon atom labels, H atoms and lattice CH_2Cl_2 omitted for clarity.

listed in Table 3. The dibenzothiophene backbone is slightly distorted in response to the oxidation and hybridization change of the sulfur atom. This is indicated by the torsion angle between the two aromatic rings: C4–C5–C6–C7, 7.2(4)°. The P=O bond vectors are rotated out of the dibenzothiophene backbone in opposite directions, and the $P=O_{av}$ bond length, 1.489 ± 0.005 Å, is indistinguishable from that in **8**, 1.491 ± 0.002 Å.

The $C–S_{av}$ bond length, 1.769 ± 0.002 Å, is slightly elongated compared to that for **8**, 1.755 ± 0.002 Å, and is indistinguishable from the average distance, 1.764 ± 0.001 Å, in dibenzothiophene-5,5-dioxide.[53] The $S=O_{av}$ bond length, 1.438 ± 0.002 Å, and the O3–S–O4 angle, 116.80(12)°, are indistinguishable from the corresponding bond length and bond angle in dibenzothiophene-5,5-dioxide, 1.439(3) Å and 117.3(3)°.[53]

The related sulfone, 4,6-bis(diphenylphosphinoyl)-dibenzothiophene-5,5-dioxide, **10**, was prepared in a one-pot synthesis, as summarized in Scheme 1, by reaction of dibenzothiophene with an *n*-BuLi/TMEDA solution followed by treatment with Ph_2PCl. The putative intermediate, 4,6-$[Ph_2P]_2$DBT, was treated, without isolation, with an excess of *m*-CBPA, resulting in the oxidation of both the phosphorus and the sulfur atoms.[54] Compound **10** was isolated as a white solid in 49% yield. The formation of the sulfone is supported by HRMS analysis that shows high-intensity $[M + H^+]$, $[M + Na^+]$, and $[M + K^+]$ ions. The IR spectrum displays strong

dx.doi.org/10.1021/ic500471w | Inorg. Chem. 2014, 53, 5698–5711

absorptions at 1331, 1196, and 1159 cm^{-1} that are tentatively assigned to $\nu_{S=O(as)}$, $\nu_{P=O}$, and $\nu_{S=O(s)}$ stretching modes, respectively. The ^{31}P NMR spectrum contains a single resonance, δ 27.7 ($CDCl_3$), δ 32.0 (d_4-MeOH) similar to the shift reported for the DBF analogue, 4,6-bis-(diphenylphosphinoyl)dibenzofuran, **2**: δ 25.2 ($CDCl_3$).[42] The ^1H and $^{13}C\{^1H\}$ NMR spectra are consistent with the proposed structure, and the shifts are similar to those reported for **2**.[42] Single-crystal X-ray diffraction analysis of **10**, cocrystallized with $CHCl_3$, confirmed the composition, and a view of the molecule and selected bond lengths are presented in Figure 3 and Table 3, respectively. Unfortunately, the

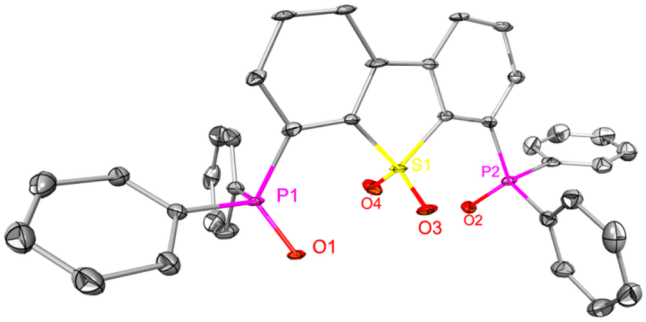

Figure 3. Molecular structure of 4,6-$[Ph_2P(O)CH_2]_2DBT(O)_2 \cdot 3CHCl_3$, **10**·$3CHCl_3$, (thermal ellipsoids, 50%) with carbon atom labels, H atoms, and lattice $CHCl_3$ omitted for clarity.

refinement of the structure is marginal due to instability of the crystals from solvent loss. X-ray diffraction analysis with crystals obtained by slow evaporation of a CH_2Cl_2/MeOH (9:1) solution did not provide improved results. Nonetheless, the $P{=}O_{av}$ bond length, 1.488 ± 0.003 Å, and S=O bond length, 1.439(4) Å, are similar to the bond lengths in **9**.

Ligand Computational Modeling. As thoroughly described in a prior report on phosphine oxide decorated DBF ligands,[42] ligand strain free energies, derived from molecular mechanics (MM) computations on 1:1 Ln(III)/ligand complexes, absent of competing inner sphere anions and solvent molecules, provide useful assessments of preferred ligand chelate docking structures.[55−57] Extending this treatment to the current set of phosphine oxide decorated DBT-based ligands, the strain energetics for **8**, **9**, and **10** on the medium-sized lanthanide Eu(III) were evaluated. The inherently weak donor ability of the S atom in the dibenzothiophene platform and hard−soft acid−base (HSAB) principles[58] portend that **8** would bind to Ln(III) ions with only its two pendent phosphine oxide O atoms. Evaluation of the relative strain free energy (G) per coordinated O atom for the geometry-optimized bidentate $O_PO'_{P'}$ structure in $[Eu(\mathbf{8})^{3+}]$, shown in Figure 4a, provides a value of 1.47 kcal mol^{-1}/donor group, and the nonbonded S atom in this structure resides 3.74 Å from the Eu(III) center. Therefore, the low strain energy, which is slightly smaller than that calculated for the DBF analogue **3** (R = Ph) in a bidentate chelate condition, 1.60 kcal mol^{-1}/donor,[59] is also consistent with **8** adopting a bidentate $O_PO'_{P'}$ chelate structure. The sulfone derivative **9** offers possibilities of forming bidentate $O_PO'_{P'}$ or O_PO_S as well as tridentate $O_PO_SO'_{P'}$ chelate structures, and the energy-minimized tridentate structure is shown in Figure 4b. The computed relative strain free energy, 0.91 kcal mol^{-1}/donor group is small, and this augurs well for tridentate docking. For

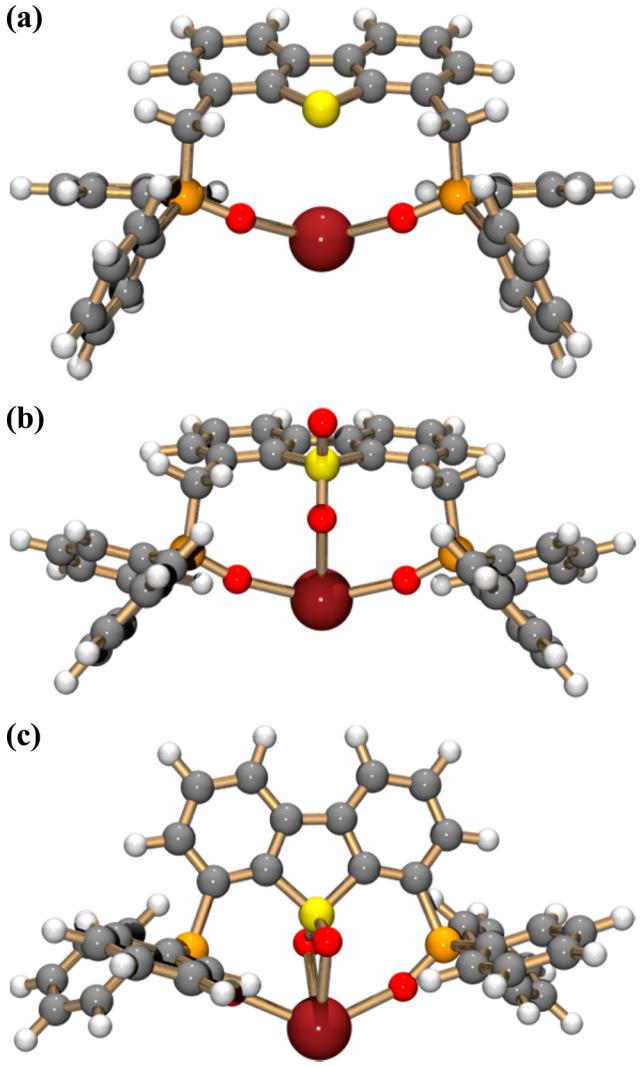

Figure 4. Geometry-optimized structures for selected maximally O-donor atom bonded ligands in gas phase, $[Eu(L)^{3+}]$ complexes: (a) ligand **8**, (b) ligand **9**, and (c) ligand **10**.

comparison, the computed value for tridentate $O_PO_NO'_{P'}$ docking by 2,6-bis(diphenylphosphinoylmethyl)pyridine *N*-oxide (TPhNOPOPO, **11**) is 1.27 kcal mol^{-1}/donor, and this ligand routinely adopts tridentate chelate structures with Ln(III) ions.[4−13] The latter also displays efficient solvent extraction properties. Lastly, the docking preference for **10** was evaluated. Here, bidentate $O_PO'_{P'}$ and O_PO_S, as well as tridentate $O_PO_SO'_{P'}$ coordination conditions are available, but the lowest strain energy condition is found for a novel $O_PO_SO'_SO'_{P'}$ tetradentate structure shown in Figure 4c. This structure provides a strain energy value of 1.93 kcal mol^{-1}/donor group, which is comparable to the strain energy (1.85 kcal mol^{-1}/donor group) for **2** acting as a bidentate $O_PO'_{P'}$ chelating ligand. Interestingly, the energy-minimized tridentate structure is actually found to be 7.4 kcal mol^{-1} higher in strain energy than the tetradentate structure. In summary, it can be expected that ligand strain should not preclude the formation of chelate structures with maximal denticity interactions by **9** and **10**.

Lanthanide Coordination with Ligand 4,6-$[Ph_2P(O)CH_2]_2$DBT (8). On the basis of our previous study with DBF analogues,[42] HSAB principles, and the molecular modeling

dx.doi.org/10.1021/ic500471w | Inorg. Chem. 2014, 53, 5698−5711

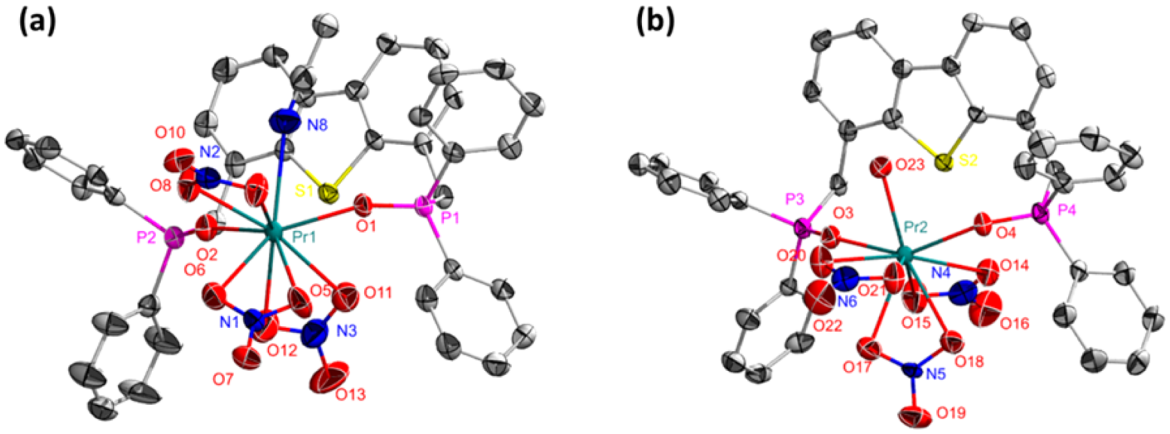

Figure 5. Molecular structure of {[Pr(**8**)$(NO_3)_3$(MeCN)]·[Pr(**8**)$(NO_3)_3(H_2O)$]}·3MeCN: (a) [Pr(**8**)$(NO_3)_3$(MeCN)] and (b) [Pr(**8**)$(NO_3)_3(H_2O)$]·(thermal ellipsoids, 50%) with carbon atom labels, H atoms, and lattice MeCN omitted for clarity.

results described above, it was expected that **8** would most likely form 1:1 and perhaps 2:1 ligand/metal complexes with Ln(III) ions utilizing only bidentate $O_PO'_{P'}$ chelate interactions with no involvement of the DBT S atom in forming the coordination field. Complexes, prepared from equimolar combinations of **8** with $Ln(NO_3)_3{\cdot}xH_2O$ (Ln = La, Pr) in MeOH (23 °C, 1 h) followed by evaporation of the volatiles, were isolated as colorless and green powders, respectively. Elemental analysis (CH) for the Pr complex shows good agreement with a 1:1 composition, [Pr(**8**)$(NO_3)_3(H_2O)$]. The FTIR spectra for several complexes are essentially identical; they show a strong absorption at 1140 cm^{-1}, tentatively assigned to $\nu_{P=O}$, that corresponds to a down-frequency coordination shift, $\Delta\nu$ = 48 cm^{-1}, compared to the free ligand. Further, the complexation of La(III) with **8** (1−4 equiv) was followed by ^{31}P and ^{1}H NMR in d_4-MeOH. The spectra show a single resonance with very small shift displacement as the ligand concentration increases, consistent with the formation of a single complex undergoing rapid ligand exchange. Since these data do not unambiguously identify the ligand denticity, single crystals of the 1:1 Pr/complex were grown by dissolution of the crude powder [Pr(**8**)$(NO_3)_3(H_2O)$] in a mixture of MeCN/MeOH (4:1) followed by slow evaporation of the solution. Single-crystal X-ray diffraction analysis revealed the formation of two chemically distinguishable complexes cocrystallized with three molecules of MeCN, resulting in an overall composition of {[Pr(**8**)$(NO_3)_3$(MeCN)]·[Pr(**8**)$(NO_3)_3(H_2O)$]}·3MeCN. Views of the independent complex units are shown in Figure 5a,b, and selected bond lengths are listed in Table 4. As anticipated, each Pr(III) ion coordinates with one *bidentate* $O_PO'_{P'}$ chelating ligand, three bidentate nitrate anions, and either an O-bonded water or N-bonded acetonitrile molecule forming nine-member inner coordination spheres. As expected, the S atoms are nonbonded with separations of Pr1···S1 3.351(1) Å and Pr2···S2 3.300(1) Å.[60] As observed in the related complex containing the DBF ligand, [Pr(**3**)$(NO_3)_3$(MeCN)], the bidentate chelate interaction in [Pr(**8**)$(NO_3)_3$(MeCN)] is slightly asymmetric as indicated by the bond lengths Pr1−O1 2.365(3) Å and Pr1−O2 2.339(3) Å. The chelate interaction is more symmetrical in the second unit, [Pr(**8**)$(NO_3)_3(H_2O)$]: Pr2−O3 2.367(3) Å and Pr2−O4 2.364(3) Å. In this complex the coordinated water molecule is hydrogen bonded with two of the lattice acetonitrile molecules: (O23−H23B 0.83(2) Å, N9···H23B 2.20(3) Å, O23···N9 2.981(7) Å, O23−H23B···N9 156.0°; O23−H23C 0.83(2) Å, N7#1···H23C 2.08 (3) Å, O23···N7#1 2.868(6) Å, O23−H23C···N7#1 157.0°. The four P═O bond lengths (P═O_{av} = 1.506 ± 0.004 Å) are identical within 3σ of the estimated standard deviations, and they are elongated relative to the free ligand bond length. It is also noted that attempts to isolate and structurally characterize complexes with 2:1 ligand/metal compositions were unsuccessful.

Lanthanide Coordination with 4,6-[$Ph_2P(O)CH_2$]$_2$DBT-(O)$_2$ (9). The coordination chemistry of **9** with $Ln(NO_3)_3{\cdot}xH_2O$ (Ln = La, Pr, Eu, Dy, Er, Lu) was studied using 1:1 and 2:1 ligand/metal combining ratios in MeOH and/or in MeOH/EtOAc (4:1), and the resulting complexes were isolated as powders after evaporation of the volatiles. Elemental analyses (CHN) for the 1:1 La(**9**) and Pr(**9**) complexes are consistent with compositions La(**9**)$(NO_3)_3(H_2O)_5$ and Pr(**9**)$(NO_3)_3(H_2O)_4$, respectively. Once more, the FTIR spectra for the isolated powders suggest phosphine oxide binding to the Ln(III) ions, but they do not provide unambiguous assignment for the ligand denticity due in part to overlapping adsorptions. For example, the strong band at 1194 cm^{-1} assigned to the $\nu_{P=O}$ stretching mode for the free ligand disappears in the spectra for the complexes, but the expected down-frequency shifted $\nu_{P=O}$ absorption is not clearly resolved from a broad adsorption centered at 1152 cm^{-1}. In addition, the spectra display two very broad bands centered at 1285 ± 4 cm^{-1} and 1152 ± 3 cm^{-1} that are tentatively assigned to $\nu_{S=O(as)}$ and $\nu_{S=O(sy)}$, and these are relatively unperturbed compared to the free ligand frequencies. However, it is noted that the $\nu_{S=O(as)}$ band falls in a region that also contains adsorptions due to nitrate modes; therefore, coordination shifts in the S═O stretching modes cannot be determined with certainty. The ^{31}P NMR spectra for d_4-MeOH solutions with 4:1, 2:1, and 1:1 **9**/La combining ratios each display a single resonance at 35.2, 36.1, and 37.2 respectively, shifted slightly from the free ligand resonance ($\Delta\delta$ 1.2−3.2) consistent with rapid ligand exchange. Crystal structure determinations were undertaken for two 1:1 complexes (La and Er) obtained by dissolution of the initially formed powders in a mixture of MeCN/MeOH 9:1 followed by slow evaporation of the homogeneous solutions. The crystal structure determination for the lanthanum complex reveals a composition [La(**9**)$(NO_3)_3(H_2O)$] in which one nitrate anion and the inner sphere water molecule are disordered over two positions.[61] Additional outer-sphere solvent molecules (likely water and/or methanol) are disordered and could not be adequately modeled. Hence, they were treated using the

dx.doi.org/10.1021/ic500471w | *Inorg. Chem.* 2014, 53, 5698−5711

Table 4. Selected Bond Lengths (Å) for Coordination Complexes

bond type	{[Pr(8)$(NO_3)_3$(MeCN)]·[Pr(8)$(NO_3)_3(H_2O)$]}·3MeCN	[La(9)$(NO_3)_3(H_2O)$]	[Er(9)$(NO_3)_3$]·2MeCN	{[Eu(9)$(Cl)_3]_2(\mu$-9)}·5MeCN	[Pr(10)$(NO_3)_3(MeOH)_2$]·MeOH
				Eu1−O3 2.358(3)	
M−O(P)	Pr1−O1 2.365(3)	La1−O1 2.469(3)	Er1−O7 2.244(2)	Eu1−O4 2.360(3)	Pr1−O1 2.4390(9)
	Pr1−O2 2.339(3)	La1−O2 2.503(3)	Er1−O9 2.256(2)	Eu1−O11 2.363(3)	
	Pr2−O3 2.367(3)			Eu2−O7 2.342(3)	
	Pr2−O4 2.364(3)			Eu2−O8 2.302(3)	
				Eu2−O12 2.338(3)	
M−O(S)		La1−O3 2.615(3)	Er1−O10 2.329(1)	Eu1−O1 2.572(3)	Pr1−O3 2.6245(9)
				Eu2−O5 2.674(3)	
M−X_{anion} (av)	2.58 ± 0.06	2.62 ± 0.06[a]	2.44 ± 0.05	2.70 ± 0.05	2.58 ± 0.06
range	2.541(4)−2.647(3)	2.564(4)−2.659(4)	2.394(2)−2.486(2)	2.662(1)−2.756(1)	2.526(1)−2.640(1)
M−$X_{(solvent)}$	Pr1−N8 2.726(5)	La1−O14 2.520(8)			Pr1−O14 2.4696(11)
	Pr2−O23 2.490(4)	La1−O14A 2.532(18)			Pr1−O15 2.5125(12)
P−O	P1−O1 1.504(3)	P1−O1 1.495(3)	P1−O7	P1−O4 1.494(3)	P1−O1 1.4992(10)
	P2−O2 1.503(3)	P2−O2 1.492(3)	1.500(2)	P2−O3 1.491(4)	P2−O2 1.4902(10)
	P3−O3 1.510(3)		P2−O9 1.502(2)	P3−O7 1.493(3)	
	P4−O4 1.508(3)			P4−O8 1.488(4)	
				P5−O11 1.501(3)	
				P6−O12 1.501(3)	
S−O(M)		S1−O3 1.452(3)	S1−O10 1.453(2)	S1−O3 1.445(3)	S1−O3 1.4520 (9)
				S2−O5 1.439(3)	
S−O		S1−O4 1.440(3)	1.431(2)		S1−O4 1.4337 (9)

[a]Disordered nitrate O atoms excluded.

dx.doi.org/10.1021/ic50047w | Inorg. Chem. 2014, 53, 5698−5711

SQUEEZE procedure.[49] A view of the 10-coordinate inner sphere complex is shown in Figure 6, and selected bond lengths

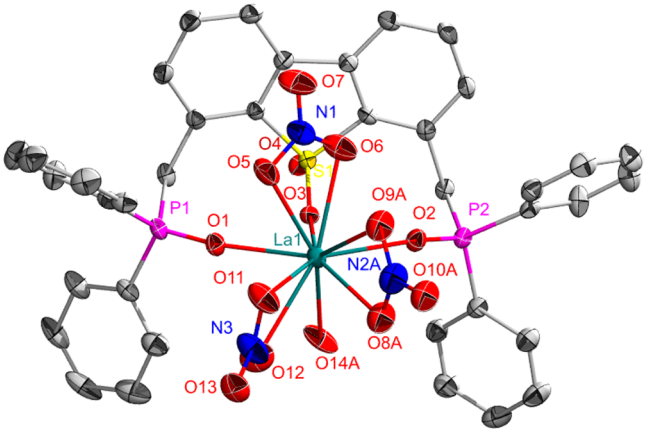

Figure 6. Molecular structure of $[La(\mathbf{9})(NO_3)_3(H_2O)]$ (thermal ellipsoids, 50%), with carbon atom labels and H atoms omitted for clarity.

are summarized in Table 4. Clearly, as predicted by the steric modeling analysis, the ligand **9** is bonded to La(III) in a *tridentate* $O_PO_SO'_{P'}$ fashion with ligand/La bond lengths La–O_P 2.469(3), La–$O'_{P'}$ 2.503(3), and La–O_S 2.615(3) Å. The remaining positions in the La(III) inner sphere are occupied by three bidentate nitrate anions and a water molecule.

Single crystals for the erbium complex, $[Er(\mathbf{9})(NO_3)_3]\cdot$ 2MeCN, were also obtained, and, in this case, recrystallization of the crude complex from MeCN/MeOH resulted in complete displacement of water from both the inner and outer coordination spheres. A view of the structure is provided in Figure 7. The $[Er(\mathbf{9})(NO_3)_3]$ unit is cocrystallized with two

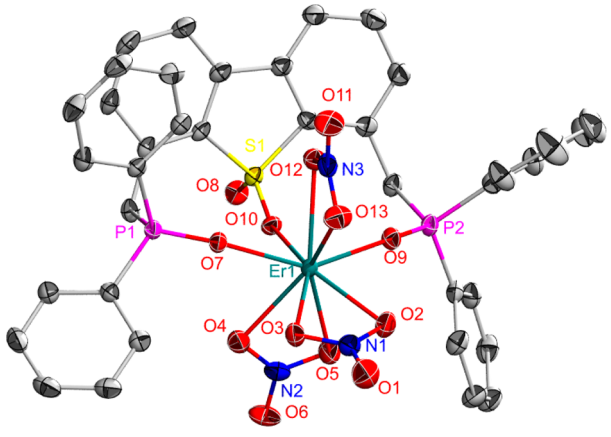

Figure 7. Molecular structure of $[Er(\mathbf{9})(NO_3)_3]\cdot$2MeCN (thermal ellipsoids, 50%) with carbon atom labels, H atoms, and outer-sphere MeCN omitted for clarity.

outer-sphere MeCN molecules, and the nine-vertex Er(III) inner-sphere environment is composed of O atoms from a *tridentate* $O_PO_SO'_{P'}$ bonded ligand **9** with [Er–O_P 2.2436(15) and 2.2557(15) Å and Er–O_S 2.3290(14) Å] and three bidentate nitrate anions. The absence of an inner-sphere solvent molecule and reduced Er(III) coordination number are consistent with the smaller size of the Er(III) cation.

Attempts to isolate and characterize 2:1 complexes of **9** with $Ln(NO_3)_3$ salts from various solvents were unsuccessful, and similar efforts with $LnCl_3$ salts produced complexes that contain weakly bound solvent molecules that complicate analysis and crystal growth. However, in one case, the combination of excess **9** with $EuCl_3\cdot 6H_2O$ produced a powder that readily lost lattice solvent in vacuo, and the resulting solid gave satisfactory elemental analysis consistent with a composition of $\{[Eu(\mathbf{9})Cl_3]_2(\mathbf{9})\}$. The IR spectrum for the solid showed strong, broad absorptions centered at 1290 cm^{-1} ($\nu_{S=O(as)}$) and 1157 cm^{-1} ($\nu_{S=O(sy)} + \nu_{P=O}$). Slow evaporation of a MeOH/MeCN solution of the powder provided single crystals, and the crystal structure determination revealed a solvated composition of $\{[Eu(\mathbf{9})(Cl)_3]_2(\mu\text{-}\mathbf{9})\}\cdot$5MeCN with the two $[Eu(\mathbf{9})(Cl)_3]$ units bridged by another molecule of **9**. A view of the structure is shown in Figure 8. The bridging interaction employs the phosphine oxide atoms: Eu1–O11 2.363(3), P5–O11 1.501(3), and Eu2–O12 2.338(3), P6–O12 1.501(3) Å. The two $[Eu(\mathbf{9})(Cl)_3]$ units are compositionally equivalent and oriented *trans* to each other across the $DBT(O)_2$ plane. Each Eu(III) inner-sphere coordination polyhedron is seven-coordinate formed by the O atoms from a tridentate $O_PO_SO'_{P'}$ chelating ligand **9**, a bridging O_P atom, and three chlorides. However, the metrical parameters in the two units differ significantly. The geometry about Eu1 is more symmetric with the Eu–O_P bond lengths, Eu1–O4 2.358(3) and Eu–O3 2.360(3) Å, indistinguishable from the bridging Eu–O_P interaction, Eu1–O11, while the Eu–O_S bond length, Eu1–O1 2.572(3) Å, is longer. The second unit is more asymmetric with Eu2–O8 2.302(3) and Eu2–O7 2.342(3) Å, the latter indistinguishable from the bridging distance, Eu2–O12. The distance involving the sulfone O atom, 2.674(3) Å, is significantly longer than it is in the first unit. Various attempts to drive these complexes to a mononuclear 2:1 composition have so far failed.

Lanthanide Coordination with 4,6-$[Ph_2P(O)]_2DBT(O)_2$ (10). The lanthanide coordination chemistry with the more rigid ligand **10** was examined using 1:1 and 2:1 ligand/Ln combining ratios (Ln = La, Pr, Eu, Dy, Er) in MeOH or $CHCl_3$/MeOH (9:1). The complexes were isolated as powders after evaporation of the volatiles. The FTIR spectra recorded from these samples typically display a broad band assigned to $\nu_{S=O(as)}$ centered in the region of 1304 ± 6 cm^{-1} ($\Delta\nu_{av}$ = 29 cm^{-1}). The $\nu_{P=O}$ stretch of the free ligand is absent in the spectra of the complexes, and a second broad band appears centered in the region of 1154 ± 3 cm^{-1}. This likely corresponds to overlapped $\nu_{P=O}$ and $\nu_{S=O(s)}$ modes. In one exception, the spectrum for the 1:1 **10**/Pr complex contains two resolved bands in this region: 1169 and 1151 cm^{-1} for the crude complex and 1174 and 1153 cm^{-1} for isolated crystals. The ^{31}P NMR spectra in d_4-MeOH display single resonances at 33.6, 34.2, and 34.5 for solutions containing ligand/metal ratios 4:1, 2:1, and 1:1, respectively, shifted downfield 1.6 to 2.5 ppm, relative to the free ligand. The ^1H NMR spectrum for the 1:1 complex is relatively unperturbed compared to the free ligand.

Single crystals for the praseodymium complex were obtained by dissolution of a powder sample described above in MeCN/MeOH (9:1) followed by slow evaporation of the solution. The X-ray structure determination reveals a composition of $[Pr(\mathbf{10})(NO_3)_3(MeOH)_2]\cdot$MeOH. A view of the structure is shown in Figure 9, and selected bond lengths are listed in Table 4. The Pr(III) ion is ten-coordinate with the coordination positions occupied by the O atoms from a *bidentate* ligand **10** bonded in an unexpected bidentate O_PO_S chelating mode, the O atoms of three bidentate nitrate anions, and the O atoms

dx.doi.org/10.1021/ic500471w | Inorg. Chem. 2014, 53, 5698–5711

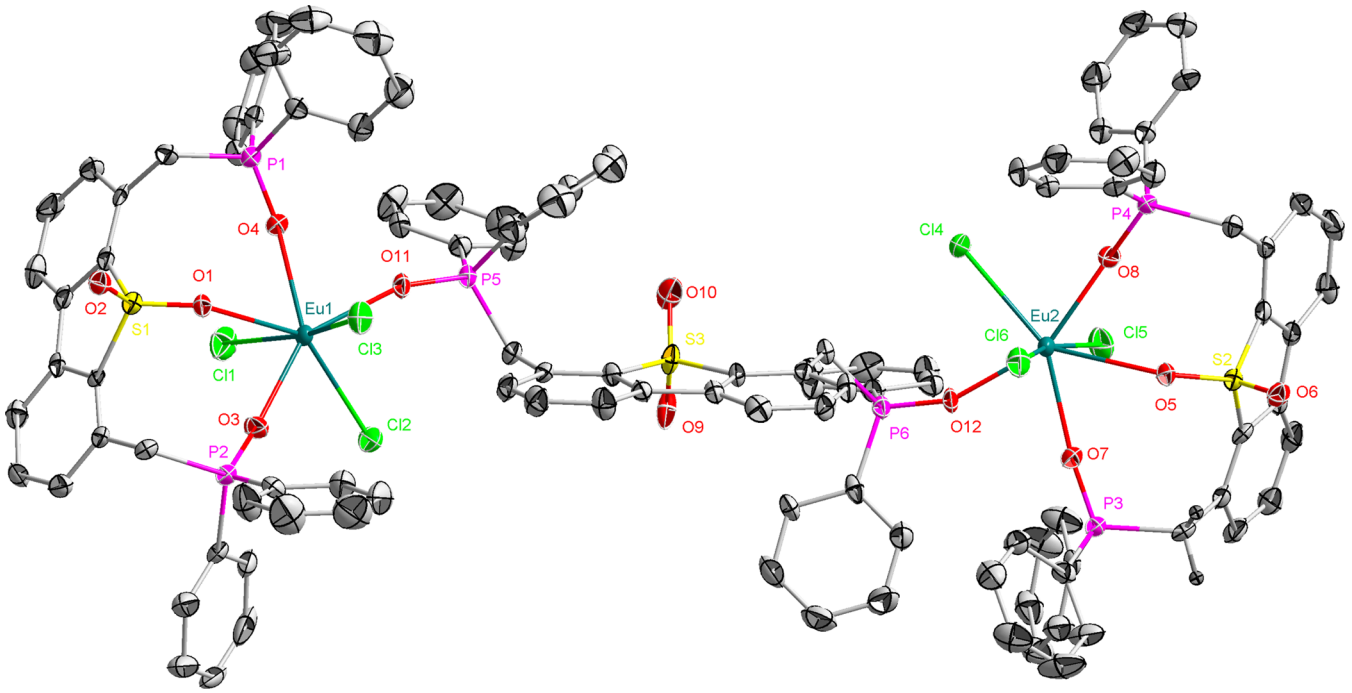

Figure 8. Molecular structure of {[Eu(**9**)$(Cl)_3]_2(\mu$-**9**)}·5MeCN (thermal ellipsoids, 50%) with carbon atom labels, H atoms, and outer-sphere MeCN omitted for clarity.

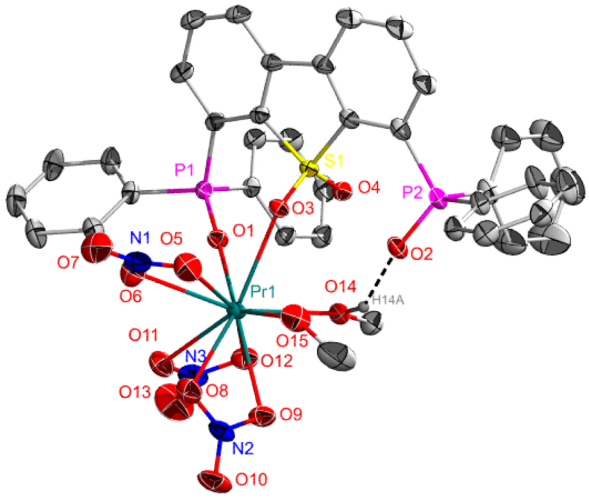

Figure 9. Molecular structure of [Pr(**10**)$(NO_3)_3(MeOH)_2$]·MeOH (thermal ellipsoids, 50%) with carbon atom labels, H atoms except hydrogen bond donor (H14A), and outer-sphere MeOH omitted for clarity.

from two inner-sphere molecules of MeOH. The second phosphine oxide group, P2−O2, is hydrogen bonded with one of the Pr-coordinated MeOH molecules (O14···O2 2.684(2) Å, O2−H14A−O14 142.0°). The unit cell also contains an outer-sphere MeOH that is hydrogen bonded with one nitrate anion and one coordinated MeOH. The bidentate chelate condition adopted by **10** may reflect the higher strain energy computed for this ligand and the hydrogen bonding between O2 and the bound methanol molecule.

Solvent Extraction Analyses. In addition to exploring the coordination chemistry of **8**, **9**, and **10** it was of interest to survey the solvent extraction performance of these new ligand classes to identify structure types that might be of use in f-element separations. In practical solvent extraction processes it is necessary to employ extractants that are soluble in a hydrocarbon diluent, for example, dodecane. This typically requires the placement of lipophilic substituents, for example, *n*-octyl, 2-ethylhexyl, on the ligand to achieve good solubility and phase separation performance. Unfortunately, this often complicates the extractant synthesis and purification. Therefore, survey extraction studies aimed at identifying potentially useful extractant types are initially accomplished with more easily prepared and purified phenyl substituted ligands that are soluble in less process-desirable chlorocarbon solvents. Consistent with this, the acid dependencies of distribution ratios, $D = [M_{org}]/[M_{aq}]$, for europium(III) and americium(III) in nitric acid solutions in contact with 10 mM solutions of phenyl-substituted **9** and **10** in 1,2-dichloroethane (DCE) were measured. The resulting data are displayed in Figure 10 along with data for two phosphine oxide decorated dibenzofurans, **2** and **3** (R = Ph)[42] and data for the classic CMPO extractant, OPhDiBCMPO, **4**, all recorded under identical conditions. Unfortunately, the stability of **8** toward aqueous nitric acid solutions is limited; therefore, distribution data for it are not included. Each ligand, except **10**, shows a general trend of increasing *D* values with increasing nitric acid concentration. The *D* values for **3** and **9** are similar in the acid range of 0.01−1 M and smaller, at all acid concentrations, than the *D* values for the CMPO ligand **4**. As noted in our prior study,[42] the *D* values for **2** are more comparable with those for **4**, and the improved performance for **2** relative to **3** was attributed to better O_P-donor group lone pair vector convergence upon formation of bidentate $O_PO'_{P'}$ complexes by **2**.[42] Since the computed ligand steric strain for **9** in a 1:1 tridentate $O_PO_SO'_{P'}$ complex is low, the donor strength of the sulfone O atoms is expected to be greater than that for the furan O atom in **2** and **3**, and the donor group vector convergence is favorable, it was expected that extraction performance for **9** would be good. However, the rather modest performance of **9** relative to that of **2**, **3**, and **4** suggests that other features may be operative. These may

dx.doi.org/10.1021/ic500471w | Inorg. Chem. 2014, 53, 5698−5711

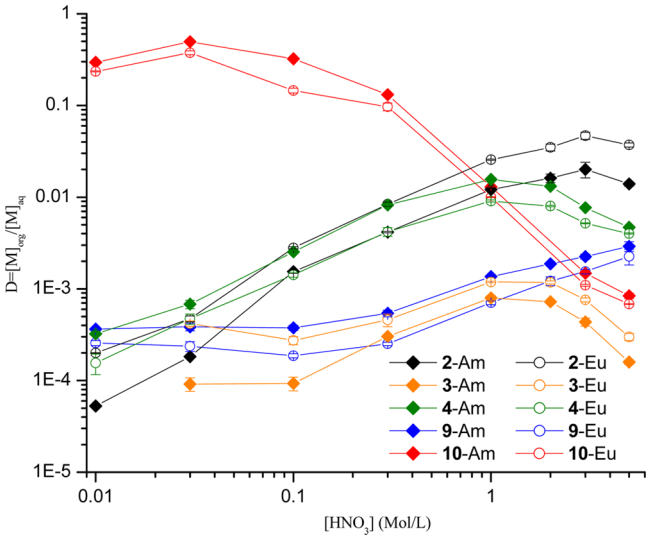

Figure 10. Americium and europium distribution ratios as a function of the initial nitric concentration. Organic phase: **2**, **3**, **4**, **9**, or **10** at 10 mM in 1,2-DCE. Aqueous phase: trace Am and 0.1 mM of europium nitrate in nitric acid. O/A = 1, T = 25 °C.

include incomplete phase transfer of the extraction complexes due to limited solubility under extraction conditions and/or formation of only a 1:1 ligand/metal complex under extraction conditions. Detailed, comparative ligand dependency studies for extractions by each ligand are required to address the latter point, and these studies will be undertaken with substituent-modified ligands soluble in dodecane solutions.

The acid dependency behavior for extractions performed with **10** is interesting in that, in the nitric acid concentration range of 0.01−0.7 M, this ligand acts as the strongest extractant of the set. The large D values, at low nitric acid concentration, are consistent with strong ligand binding resulting from tridentate $O_PO_SO'_{P'}$ chelation or perhaps from the tetradentate interaction predicted in the modeling analysis. The decrease in D values at higher acid concentrations (>0.1 M) likely results from competitive extraction of nitric acid by the ligand. This point and ligand dependency analyses will be explored further with a hydrocarbon-soluble derivative of **10**. Lastly, typical of most O-donor extractants, both **9** and **10**, like OPhDiBCMPO, extract Am with a very small preference over Eu at all acid concentrations (separation factor $SF_{Am/Eu}$ < 2 at 3 M HNO_3). Interestingly, the DBF analogues, **2** and **3**, show the opposite preference,[42] and this feature will continue to be examined as additional studies are undertaken.

CONCLUSION

Efficient syntheses for the multifunctional phosphine oxide decorated ligands **8**, **9**, and **10**, based upon dibenzothiophene and dibenzothiophene sulfone platforms, were developed; the new ligands were spectroscopically characterized, and their molecular structures were verified by single-crystal X-ray diffraction techniques. Molecular modeling of potential strain-free chelate binding modes of the ligands on a medium-sized lanthanide ion, Eu(III), were completed, and the coordination chemistry with selected lanthanide nitrates was explored. In the case of **8**, the computations suggested that, based upon steric strain, this ligand should coordinate utilizing a bidentate $O_PO'_{P'}$ binding mode with the dibenzothiophene S atom remaining nonbonded toward the lanthanide ion. An X-ray crystal structure determination for one complex, $\{[Pr(\mathbf{8})(NO_3)_3(MeCN)]\cdot[Pr(\mathbf{8})(NO_3)_3(H_2O)]\}\cdot 3MeCN$, confirmed this expectation. Similar behavior was previously observed for the related DBF ligand, **3**. On the other hand, computations for the sulfone ligand **9** indicated a preference for tridentate $O_PO_SO'_{P'}$ chelate binding, and subsequent studies of the coordination chemistry of **9** with $Ln(NO_3)_3$ salts showed formation of 1:1 complexes with the anticipated tridentate $O_PO_SO'_{P'}$ chelate interaction. Attempts to isolate 2:1 complexes that might be expected to form in a ligand-rich extraction environment were not successful. However, combination of excess **9** with $EuCl_3$ produced a complex, $\{[Eu(\mathbf{9})(Cl)_3]_2(\mu\text{-}\mathbf{9})\}$, in which two $[Eu(\mathbf{9})Cl_3]$ units, with **9** bonded in a tridentate chelate fashion, are bridged by another molecule of **9** bonded through Eu−O═P interactions.

Molecular modeling of the potential interactions available with the more sterically constrained ligand **10** revealed that a unique tetradentate $O_PO_SO'_SO'_{P'}$ chelate structure was sterically accessible and strain energy favored. However, a lanthanide complex utilizing this bonding mode has not yet been isolated. In one structurally characterized complex, $[Pr(\mathbf{10})(NO_3)_3(MeOH)_2]\cdot MeOH$, the ligand was observed to be coordinated via an O_PO_S bidentate interaction. These initial observations indicate that the coordination chemistry of **8**, **9**, and **10** is rich in variety, and additional aspects remain under study.

Survey solvent extraction analyses for Eu(III) and Am(III) were also undertaken to determine if the new ligand structure types displayed potentially useful separation behavior. Unfortunately, **8** displayed poor long-term stability in aqueous nitric acid solutions, and a complete survey of extraction performance was not completed. The performance of **9** indicated that this ligand is a weaker extractant than the classical OPhDiBCMPO extractant for both Eu(III) and Am(III), while the separation factors, over the acid range of 0.01−3.0 M, are comparable. Ligand **10**, on the other hand, is a much stronger extractant than **9** or the CMPO ligand in the acid range of 0.01−0.3 M. This performance is interesting, and it encourages continuing efforts to prepare a dodecane-soluble derivative and to undertake more extensive extraction analyses.

ASSOCIATED CONTENT

Supporting Information

Selected IR, HRMS, vis−UV, and NMR spectra and CIF files for the crystal structures. This material is available free of charge via the Internet at http://pubs.acs.org.

AUTHOR INFORMATION

Corresponding Author

*E-mail: rtpaine@unm.edu.

Notes

The authors declare no competing financial interest.

ACKNOWLEDGMENTS

Financial support for this study at the University of New Mexico was provided by the U.S. Department of Energy (DOE), Office of Basic Energy Sciences (BES), Division of Chemical Sciences, Geosciences, and Biosciences (Grant DE-FG02-03ER15419 (R.T.P)). In addition, funds from the National Science Foundation assisted with the purchases of the X-ray diffractometer (CHE-0443580) and NMR spectrometers (CHE-0840523 and −0946690). Support for liquid−

liquid extraction (L.D.H.) and molecular modeling (B.P.H) studies at Oak Ridge National Laboratory was provided by the DOE, Office of Science, BES, Chemical Sciences, Geosciences, and Biosciences Division.

REFERENCES

(1) McCabe, D. J.; Russell, A. A.; Karthikeyan, S.; Paine, R. T.; Ryan, R. R.; Smith, B. *Inorg. Chem.* **1987**, *26*, 1230−1235.
(2) Conary, G. S.; Russell, A. A.; Paine, R. T.; Hall, J. H.; Ryan, R. R. *Inorg. Chem.* **1988**, *27*, 3242−3245.
(3) Russell, A. A.; Meline, R. L.; Duesler, E. N.; Paine, R. T. *Inorg. Chim. Acta* **1995**, *231*, 1−5.
(4) Rapko, B. M.; Duesler, E. N.; Smith, P. H.; Paine, R. T.; Ryan, R. R. *Inorg. Chem.* **1993**, *32*, 2164−2174.
(5) Engelhardt, U.; Rapko, B. M.; Duesler, E. N.; Frutos, D.; Paine, R. T. *Polyhedron* **1995**, *14*, 2361−2369.
(6) Bond, E. M.; Duesler, E. N.; Paine, R. T.; Neu, M. P.; Matonic, J. H.; Scott, B. L. *Inorg. Chem.* **2000**, *39*, 4152−4155.
(7) Bond, E. M.; Duesler, E. N.; Paine, R. T.; Nöth, H. *Polyhedron* **2000**, *19*, 2135−2140.
(8) Gan, X.-M.; Duesler, E. N.; Paine, R. T. *Inorg. Chem.* **2001**, *40*, 4420−4427.
(9) Matonic, J. H.; Enriquez, A. E.; Scott, B. L.; Paine, R. T.; Neu, M. P. *Nucl. Sci. Technol.* **2002**, *3*, 100−105.
(10) Gan, X.-M.; Paine, R. T.; Duesler, E. N.; Nöth, H. *Dalton Trans.* **2003**, 153−159.
(11) Gan, X.-M.; Rapko, B. M.; Duesler, E. N.; Binyamin, I.; Paine, R. T.; Hay, B. P. *Polyhedron* **2005**, *24*, 469−474.
(12) Pailloux, S.; Shirima, C. E.; Ray, A. D.; Duesler, E. N.; Paine, R. T.; Klaehn, J. R.; McIlwain, M. E.; Hay, B. P. *Inorg. Chem.* **2009**, *48*, 3104−3113.
(13) Pailloux, S.; Shirima, C. E.; Ray, A. D.; Duesler, E. N.; Smith, K. A.; Paine, R. T.; Klaehn, J. R.; McIlwain, M. E.; Hay, B. P. *Dalton Trans.* **2009**, 7486−7493.
(14) Gan, X.-M.; Binyamin, I.; Rapko, B. M.; Fox, J.; Duesler, E. N.; Paine, R. T. *Polyhedron* **2006**, *25*, 3387−3392.
(15) Gan, X.-M.; Duesler, E. N.; Parveen, S.; Paine, R. T. *Dalton Trans.* **2003**, 4704−4708.
(16) Binyamin, I.; Pailloux, S.; Duesler, E. N.; Rapko, B. M.; Paine, R. T. *Inorg. Chem.* **2006**, *45*, 5886−5892.
(17) Binyamin, I.; Pailloux, S.; Hay, B. P.; Rapko, B. M.; Duesler, E. N.; Paine, R. T. *J. Heterocycl. Chem.* **2007**, *44*, 99−103.
(18) Bond, E. M.; Engelhardt, U.; Deere, T. P.; Rapko, B. M.; Paine, R. T. *Solvent Extr. Ion Exch.* **1997**, *15*, 381−400.
(19) Bond, E. M.; Engelhardt, U.; Deere, T. P.; Rapko, B. M.; Paine, R. T. *Solvent Extr. Ion Exch.* **1998**, *16*, 967−983.
(20) Nash, K. L.; Lavallette, C.; Borkowski, M.; Paine, R. T.; Gan, X.-M. *Inorg. Chem.* **2002**, *41*, 5849−5858.
(21) Sulakova, J.; Paine, R. T.; Chakravarty, M.; Nash, K. L. *Sep. Sci. Technol.* **2012**, *47*, 1−9.
(22) Haenel, M. W.; Jakubik, D.; Rothenberger, E.; Schroth, G. *Chem. Ber.* **1991**, *124*, 1705−1710.
(23) Kranenburg, M.; van der Burgt, Y. E. M.; Kamer, P. C. J.; van Leeumen, P. W. N. M.; Govbitz, K.; Fraamje, J. *Organometallics* **1995**, *14*, 3081−3089.
(24) Vogl, E. M.; Bruckmann, J.; Krüger, C.; Haenel, M. W. *J. Organoganomet. Chem.* **1996**, *520*, 249−252.
(25) Vogl, E. M.; Bruckmann, J.; Kessler, M.; Krüger, C.; Haenel, M. W. *Chem. Ber.* **1997**, *130*, 1315−1319.
(26) Hlavinka, M. L.; Hagadorn, J. R. *Chem. Commun.* **2003**, 2686−2687.
(27) Skar, M. L.; Svendsen, J. S. *Tetrahedron* **1997**, *53*, 17425−17437.
(28) (a) Kanemasa, S.; Oderaotoshi, Y.; Yamamoto, H.; Tanaka, J.; Wada, E. *J. Org. Chem.* **1997**, *62*, 6454−6455. (b) Kanemasa, S.; Oderaotoshi, Y.; Sakaguchi, S.; Yamamoto, H.; Tanaka, J.; Wada, E.; Curran, D. P. *J. Am. Chem. Soc.* **1998**, *120*, 3074−3088.
(29) Deng, Y.; Chang, C. J.; Nocera, D. G. *J. Am. Chem. Soc.* **2000**, *122*, 410−411.
(30) Kaul, R.; Deechongkit, S.; Kelly, J. W. *J. Am. Chem. Soc.* **2002**, *124*, 11900−11907.
(31) Kuang, S.-M.; Fanwick, P. E.; Walton, R. A. *Inorg. Chem.* **2002**, *41*, 405−412.
(32) Caradoc-Davies, P. L.; Hanton, L. R. *Dalton Trans.* **2003**, 1754−1758.
(33) Pintado-Alba, A.; de la Riva, H.; Nieuwhuyzen, M.; Bautista, D.; Raithby, P. R.; Sparkes, H. A.; Teat, S. J.; López-de-Luzuriaga, J. M.; Lagunas, C. M. *Dalton Trans.* **2004**, 3459−3467.
(34) Porter, R. M.; Danopoulos, A. A. *Polyhedron* **2006**, *25*, 859−863.
(35) De la Riva, H.; Nieuwhuyzen, M.; Fierro, C. M.; Raithby, P. R.; Male, L.; Lagunas, M. C. *Inorg. Chem.* **2006**, *45*, 1418−1420.
(36) Robbins, T. A.; Cram, D. J. *J. Chem. Soc., Chem. Commun.* **1995**, 1515−1516.
(37) Agbaria, K.; Biali, S. E. *J. Org. Chem.* **2001**, *66*, 5482−5489.
(38) Li, F.; Delgado, A.; Coelho, A.; Drew, M. G. B.; Félix, V. *Tetrahedron* **2006**, *62*, 8550−8558.
(39) Li, F.; Delgado, R.; Drew, M. G. B.; Félix, V. *Dalton Trans.* **2006**, 5396−5403.
(40) Li, F.; Li, L.; Delgado, R.; Drew, M. G. B.; Félix, V. *Dalton Trans.* **2007**, 1316−1324.
(41) Han, C.; Xie, G.; Li, J.; Zhang, Z.; Xu, H.; Dend, Z.; Zhao, Y.; Yan, P.; Liu, S. *Chem.—Eur. J.* **2011**, *17*, 8947−8956.
(42) Rosario-Amorin, D.; Duesler, E. N.; Paine, R. T.; Hay, B. P.; Delmau, L. H.; Reilly, S. D.; Gaunt, A. J.; Scott, B. L. *Inorg. Chem.* **2012**, *51*, 6667−6681.
(43) Horwitz, E. P.; Kalina, D. G.; Diamond, H.; Vandegrift, G. F.; Schulz, W. W. *Solvent Extr. Ion Exch.* **1985**, *3*, 75−109.
(44) Han, C.; Zhang, Z.; Xu, H.; Yue, S.; Li, J.; Yan, P.; Deng, Z.; Zhao, Y.; Yan, P.; Liu, S. *J. Am. Chem. Soc.* **2012**, *134*, 19179−19188.
(45) The atom numbering systems used with the NMR chemical shift assignments are provided on individual spectra in the Supporting Information.
(46) Korang, J.; Grither, W. R.; McCulla, R. D. *J. Am. Chem. Soc.* **2010**, *132*, 4466−4476.
(47) *APEX 2;* Bruker AXS, Inc.: Madison, WI, 2007. (b) *SAINT + 7.01;* Bruker AXS, Inc.: Madison, WI, 2003. (c) *SADABS 2.10;* Sheldrick, G. M., Ed.; University of Gottingen: Gottingen, Germany, 2003.
(48) *SHELXL-97;* Bruker AXS, Inc.: Madison, WI, 2008.
(49) (a) van der Sluis, P.; Spek, A. L. *Acta Crystallogr.* **1990**, *A46*, 194−201. (b) Spek, A. L. *Acta Crystallogr.* **1990**, *A46*, C34.
(50) (a) Allinger, N. L.; Yuh, Y.-H.; Lii, J.-H. *J. Am. Chem. Soc.* **1989**, *111*, 8551−8566. (b) Lii, J.-H.; Allinger, N. L. *J. Am. Chem. Soc.* **1989**, *111*, 8566−8575. (c) Lii, J.-H.; Allinger, N. L. *J. Am. Chem. Soc.* **1989**, *111*, 8576−8582.
(51) Hay, B. P. *Coord. Chem. Rev.* **1993**, *126*, 177−236.
(52) *PCModel, version 9.3;* Serena Software: Bloomington, IN, 2011.
(53) Wang, C.; Dong, H.; Li, H.; Zhao, H.; Meng, Q.; Hu, W. *Cryst. Growth Des.* **2010**, *10*, 4155−4160.
(54) Han and co-workers[44] reported the formation of the P-oxidized ligand 4,6-bis(diphenylphosphinoyl)dibenzothiophene, 4,6-$[Ph_2P(O)]_2$DBT, by treatment of the putative intermediate phosphine, 4,6-$[Ph_2P]_2$DBT, with 30% H_2O_2 solution at room temperature. The formation of the P-oxidized compound, accompanied by small amounts of **10**, was confirmed in our study. However, our attempts to isolate 4,6-$[Ph_2P(O)]_2$DBT in high purity suitable for extraction analyses were unsuccessful.
(55) The established force field-based structure scoring method[56] utilized in this study seeks to identify gas phase structures with low conformational energy, low degrees of induced strain, and few restricted bond rotations. The computed relative strain free energy (G) per bonded donor group indicates the level of binding-site preorganization for the ligand on a medium-sized Eu(III).
(56) Hay, B. P.; Oliferenko, A. A.; Uddin, J.; Zhang, C.; Firman, T. K. *J. Am. Chem. Soc.* **2005**, *127*, 17043−17053.
(57) Representative examples of the application of ligand strain energies to correlate ligand structure with metal binding affinity include (a) Hay, B. P.; Rustad, J. R.; Hostetler, C. J. *J. Am. Chem. Soc.*

1993, *115*, 11158−11164. (b) Hay, B. P.; Zhang, D.; Rustad, J. R. *Inorg. Chem.* **1996**, *35*, 2650−2658. (c) Dietz, M. L.; Bond, A. H.; Hay, B. P.; Chiarizia, R.; Huber, V. J.; Herlinger, A. W. *Chem. Commun.* **1999**, 1177−1178. (d) Hay, B. P.; Dixon, D. A.; Vargas, R.; Garza, J.; Raymond, K. N. *Inorg. Chem.* **2001**, *40*, 3922−3935. (e) Lumetta, G. J.; Rapko, B. M.; Garza, P. A.; Hay, B. P.; Gilbertson, R. D.; Weakley, T. J. R.; Hutchison, J. E. *J. Am. Chem. Soc.* **2002**, *124*, 5644−5645.

(58) Pearson, R. G. *Inorg. Chem.* **1988**, *27*, 734−740.

(59) The strain energies for the two DBF ligands **2** and **3** (R = Ph) were recomputed since our initial report,[42] using a new force field. The resulting *G* per donor group values for **2** and **3** in bidentate $O_PO'_{P'}$ binding modes are 1.85 and 1.60 kcal mol^{-1}/donor group, respectively.

(60) The sum, [3.08 Å], of covalent radii Pr [2.03(7) Å] and S [1.05(3) Å] may be used to estimate a Pr−S covalent bond length. This estimate is much shorter than the computed separation in the gas phase **8**/Pr complex [3.74 Å] or the observed distances in {[Pr(**8**)$(NO_3)_3$(MeCN)]·[Pr(**8**)$(NO_3)_3(H_2O)$]}·3MeCN, and it would be beyond the expected upper limit of a S-donor/Pr(III) acceptor interaction distance. By comparison, the sum [2.69 Å] of the Pr and O [0.66(2) Å] covalent radii can be compared to the average $Pr-O_P$ coordinate bond length [2.36 ± 0.02 Å] in {[Pr(**8**)$(NO_3)_3$(MeCN)]·[Pr(**8**)$(NO_3)_3(H_2O)$]}·3MeCN. Covalent radii estimates are taken from Cordero, B.; Gómez, V.; Platero-Prats, A. E.; Revés, M.; Echeverría, J.; Cremades, E.; Barragán, F.; Alvarez, S. *Dalton Trans.* **2008**, 2832−2838.

(61) Single crystals obtained by recrystallization of the crude powder [Pr(**9**)$(NO_3)_3$]·4(H_2O) were also examined and found to suffer from crystal quality shortcomings as described for the [La(**9**)$(NO_3)_3(H_2O)$] complex. The complexes are isomorphous with disorder in one nitrate anion and the bound water molecule.